Deanship of Graduate Studies

Al-Quds University

Performance Analysis of Orthogonal Space-time Block Codes Over Nakagami-q (Hoyt) MIMO RFID Backscattering Channels

Yasmin Hisham Tawfiq Qabbani

M.Sc Thesis

Jerusalem-Palestine

1438-2017

Performance Analysis of Orthogonal Space-time Block Codes Over Nakagami-q (Hoyt) MIMO RFID Backscattering Channels

Prepared By:

Yasmin Hisham Tawfiq Qabbani

B.Sc.: Electronic Engineering from Al-Quds University, Palestine

Supervisor: Dr. Ali Jamoos

A thesis submitted in partial fulfillment of the requirements for the degree of Master of Electronic and Computer Engineering/Department of Electronic and Computer Engineering/ Faculty of Engineering/ Graduate Studies

Jerusalem-Palestine

1438-2017

Al-Quds University

Deanship of Graduate Studies

Electronics and Computer Engineering

Thesis Approval

Performance Analysis of Orthogonal Space-time Block Codes Over Nakagami-*q* (Hoyt) MIMO RFID Backscattering Channels

Prepared By: Yasmin Hisham Tawfiq Qabbani

Registration No: 21220371

Supervisor: Dr. Ali Jamoos

Master thesis submitted and accepted, Date: 10 / 5 /2017

The name and signatures of examining committee members are as follows:

1. Head of committee   Dr. Ali Jamoos   Signature: ....

2. Internal Examiner   Dr. Ahmed Abdou   Signature: ....

3. External Examiner   Dr. Mutamed Khatib   Signature: ....

Jerusalem-Palestine

1438-2017

Dedication

To my father, mother, sister, brother,

friends and all of my family

Declaration:

I certify that this thesis submitted for the degree of Master, is the result of

my own research, except where otherwise acknowledged, and that this

study (or any part of the same) has not been submitted for a higher degree

to any other university or institution.

Signed:…………………………………………
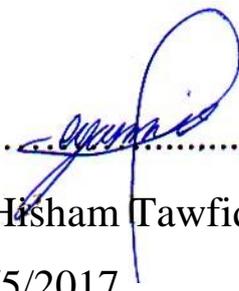
Yasmin Hisham Tawfiq Qabbani

Date: 10/5/2017

Acknowledgments

Abstract

Radio frequency identification (RFID) is an automatic identification technology which utilizes radio-frequency electromagnetic fields to identify objects carrying tags in the reading range of a reader. Such identification over a wireless channel doesn't necessitate the tag and the reader being in physical contact or line-of-sight (LOS) aligned.

This preferable feature of sending identification data wirelessly may adversely affect the performance of the RFID system, because even when LOS path exists, heavy small-scale fading may still be present due to indoor operation, a cluttered reader environment, and the inhomogeneous nature of the tagged object. To mitigate this fading problem and increase the read reliability, space-time block coding (STBC) for multiple-input multiple-output (MIMO) RFID systems is suggested and employed.

In this thesis, a performance analysis of orthogonal space-time block codes (OSTBC) in passive MIMO RFID system is conducted. More particularly, the conditional moment-generating function (MGF) approach is employed to analyse the performance of OSTBC over Nakagami-q (Hoyt) MIMO RFID backscattering channels. New exact and asymptotic closed-form symbol error rate (SER) expressions are derived for the case of two and four reader-receiving antennas ($N = 2, 4$).

The diversity order that the system can achieve is found to be L, where L is the number of tag antennas, and the performance of this channel is found to be more sensitive to the channel condition (the q parameter) of the forward link than that of the backscattering link. A good agreement with previous published studies was observed for the special case that the Hoyt fading covers.

Table of Contents

List of Figures

Chapter 1

Introduction

1.1 Motivation

RFID is a form of wireless non-contact communication that uses radio waves to automatically identify and track objects [1]. A basic RFID system is made up of three primary components: RFID readers (also known as interrogators), RFID tags (also known as labels), and a data processing subsystem [2]. The tag contains electronically stored information which can be read from up to several meters away in response to reader's interrogating radio waves. Depending on power supplying methods, RFID tags are divided into three categories, passive, active, and semi-passive (also called battery assisted passive) tags [3].

Because passive tags are the least expensive of these three types, they are commonly used in high volumes of applications. For passive RFID tags that draw energy from the reader and simply reflect back a modulated signal to it, the channel between the reader and the tag is the cascade of two fading channels, the forward and backscatter links [4]. This cascaded channel, which is characterized as a query-fading-coding-fading structure, causes deeper and more frequent small-scale fades than the conventional one-way channel resulting in lower transmission reliability and shorter read ranges [3].

Unfortunately, this poor reliability may render RFID technology practically infeasible for many application scenarios. Thus, assessment and extensive performance analysis are a necessity.

1.2 State of the Art

Few fading measurements have been conducted and reported in the literature. Fading on the signal received by the RF tag was the focus of Mitsugi and Shibao [5] [6] and Polivka *et al.* [7] studies. Others have studied fading on the signal received by the reader: Kim *et al.* [8] have presented small-scale fading statistics (the cumulative distribution functions) for short ranges in an indoor environment at 2.4 GHz, while Banerjee *et al*. [9] [10] have presented fading measurements at 915 MHz and demonstrated the importance of spatial and frequency diversity to effectively mitigate multipath fading effects.

In an effort to provide a more comprehensive view of the MIMO RF backscattering channel's behavior, extensive analysis was also performed. In [11] [12] [13] [14], researchers provided analytical bit error rate (BER) and revealed several interesting properties of the channel assuming a Rayleigh fading channel. Others studied the behavior of the channel under more general fading models; in [15] researchers analytically investigated the operating range of this MIMO structure under the Nakagami-m fading channel. In [16] the authors presented a general formulation to study orthogonal space–time block codes (OSTBCs) for RF backscattering with different fading assumptions and then analytically studied the SER performances under Rician fading and Nakagami-m fading.

1.3 Thesis Contribution

Recently, the Nakagami-q (Hoyt) model is being used frequently in performance analysis and other studies related to mobile radio communications [17] [18] [19] , and it shows good ability to describe the statistics of real-world radio channels.

This thesis proposes to extend the work done in [16] by considering Hoyt RF backscattering channels. New exact and asymptotic closed-form expressions are derived for the SER of the OSTBC over Hoyt RF backscattering channels using the conditional MGF approach [20]. Several interesting properties of this channel have been discussed: the achievable diversity order and the effects of forward and backscattering links on the SER performance.

The suitability of approximating the performance of this system with a properly chosen Nakagami-m model was also examined. A comparison with previously-published studies was conducted for the special case that the Hoyt fading covers.

1.4 Outline of the Thesis

This thesis is organized as follows: Chapter 2 describes RFID technology at an overview level. Chapter 3 discusses the fading concept and distributions types and deals with the MIMO RFID system model and related diversity techniques. Chapter 4 briefly reviews the space-time coding and introduces the conditional MGF approach used to analyse the performance of OSTBC. In addition, it presents the derivation of closed-form SER expressions of OSTBC over Hoyt fading. Numerical results are presented and discussed in Chapter 5. Finally, conclusions are drawn and future topics are suggested in Chapter 6.

Chapter 2

RFID Technology Overview

In recent years, systems employing RFID technology have been rapidly growing, and successfully applied in areas of manufacturing, supply chain, agriculture, healthcare, and services to name a few. This chapter briefly describes the RFID system, from its basic structure to its most recent applications and benefits.

2.1 RFID Systems

RFID belongs to a broad category of technologies referred to as automatic identification and data capture (AIDC). AIDC methods automatically identify objects and collect their data without manual data entry. The main difference among these technologies is in the way of storing and retrieving identification data by requiring less human intervention.

RFID methods utilize radio waves to wirelessly accomplish this identification and data-capturing process. RFID excelled in the AIDC industry through its ease, speed, agility and endurance and subsequently became a major topic of research in these current years.

The first idea behind RFID was published by Harry Stockman in 1948 [21]. In [21], he describes the antenna load modulation technique, in which, as will be detailed later, the amount of power reflected back to the RFID reader antenna can be varied by alternating the load of the RFID tag antenna. This basic concept is still being used in all RFID systems in more or less sophisticated ways.

The most common RFID system architecture consists of three key elements [22]:

- The RFID tag, or transponder, that is the small mobile unit attached to the item of interest to unequivocally identify it.

- The RFID reader, or transceiver, which queries transponders for information stored on them. Its functions could also include powering the tag and writing data to it.

- The data processing subsystem or server, which processes the data obtained from readers.

Following are the detailed discussion of each component of the RFID system.

2.1.1 RFID Tags:

Typical transponders (transmitters /responders) or RFID tags consist of an integrated circuit (IC) connected to an antenna [22]. They come in many different designs, shapes, and sizes (see examples in Figure 2.1). They may broadly be classified under three categories depending on: how the tags obtain power; the frequency at which they operate; and the various functionalities implemented on them.

Figure 2.1: Pictures of some RFID tag types

2.1.1.1 Power Source:

A tag requires power to process signals received from the reader and to send the data-encoded (either reflected or generated) signals back to it. Depending on how tags obtain the power and how they use that power, tags are classified as [23]:

- Passive tag: does not have its own power source or an active transmitter. This tag obtains a small amount of power from reader interrogating signals to energize its IC and to communicate back to the reader.

- Semi-passive tag: also called semi-active, battery-assisted passive or battery-assisted tag, this tag has an on-board battery to power its IC, but, like a passive tag, it uses backscatter to communicate with the reader.

- Active tag: has an on-board power source, usually a battery, and an active transmitter. This tag uses the battery to power its IC and transmitter. It does not need emitted power or radio signals from the reader to transmit its data.

2.1.1.2 Frequency of Operation:

RFID technology uses the radio wave portion of the electromagnetic spectrum; the entire electromagnetic spectrum includes gamma-rays, X-rays, ultraviolet light, visible light, infrared light, microwaves, and radio waves as shown in Figure 2.2.

Electromagnetic Spectrum

| Electric Waves | Radio Waves | Infra-Red | Visible Light | Ultra Violet | X-Rays | Gamma Rays | Cosmic Rays |

Radio Spectrum

9kHz 30 kHz 300kHz 3000kHz 30MHz 300MHz 3GHz 30GHz 300GHz 3000GHz

VLF | LF | MF | HF | VHF | UHF | SHF | EHF | Not designated

| 125-134 kHz | 13.56 MHz | 860-930 MHz | 2.4 & 5.8 GHz |
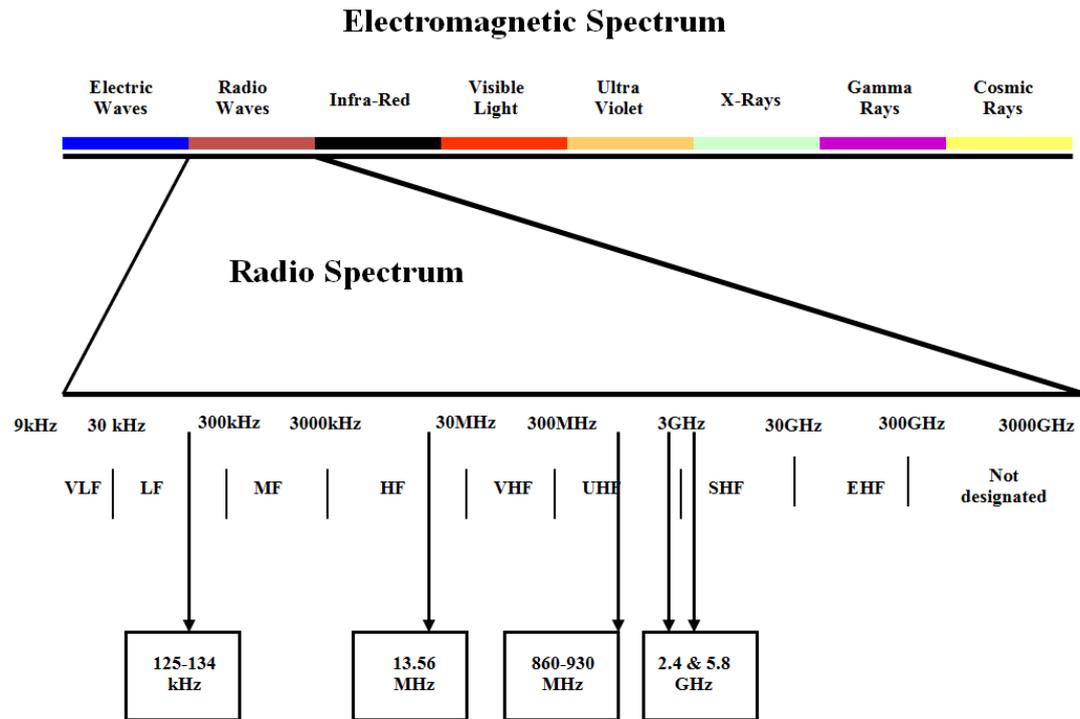
Figure 2.2: A graph of the electromagnetic spectrum with the frequency bands that the RFID systems can use [24]

Within the radio spectrum is an enormous range of frequencies. To categorize and manage the different areas of the spectrum, the radio spectrum is split into many different bands, but RFID technology uses only four: low frequency (LF), high frequency (HF), ultrahigh frequency (UHF), and microwave. The exact frequency that the tag operates in varies depending on the application and the regulations in different countries, and accordingly the maximum achievable read range varies [22].

The frequency bands and the most common RFID system frequencies are listed in Table 2.1.

Table 2.1: RFID frequency bands and the corresponding read ranges for passive tags

Range	LF	HF	UHF	Microwave
Frequency Available	30-300 KHz	3-30 MHz	300-1000 MHz	1-6 GHz
Used for RFID	125-134 KHz	13.56 MHZ	433 MHz & 860-960 MHz	2.4 & 5.8 GHz
Read Range	≈ 0.5 Meters	≈ 3 Meters	≈ 9 Meters	> 10 Meters

2.1.1.3 Functionality (EPCGlobal Classes):

EPCGlobal is leading the development of industry-driven standards for the electronic product code (EPC) to support the use of RFID systems. Depending on the tag functionality, EPCGlobal has classified RFID tags into different classes [25] [23]. The main criteria for differentiation are read/write capability, source of power, capacity of memory, and capability of communication. Table 2.2 shows this RFID tag classification.

Table 2.2: EPCGlobal tag classes

Class	Description
Class 0	Passive, Preprogrammed Read-Only IC chips
Class 0+	Passive, Write Once Read Many (WORM) IC chips, using class 0 protocols.
Class I	Passive, WORM IC chips.
Class II	Passive, Read/Write capability with memory available for user, and extras such as encryption.
Class III	Semi-passive tags with on-board environmental sensors, Read/Write capability, and memory space availability for user.

Class IV	Active with on-board sensors, Read/Write capability, user memory, and provision for peer communication with other similar active tags and interrogator.
Class V	Similar to **Class IV** tags but with additional functionality; can provide power to other tags and communicate with devices other than readers.

2.1.2 RFID Readers:

Typical transceivers (transmitters /receivers) or RFID readers are made up of primarily two components: the antenna and the interrogator circuitry [23]. The antenna is used for communication with the tag using RF waves, and, as discussed before, it could also be used to power the tags ICs for passive tags.

The interrogator circuitry is an intermediary between the reader antenna and the data processing subsystem. It's responsible for sending data through the reader antenna and then receiving and forwarding it to the back end for processing through a wireless or wired channel. By doing so, readers delegate most of the computational effort to other computationally more powerful devices and they are kept as simple as possible. Interrogator circuitry also coordinates between different reader antennas for the efficient and successful reading of tags [23].

Readers come, like tags, in a large number of different sizes and features. For examples they can be handheld, mobile, or affixed in a stationary position, and they can issue two types of challenge: multicast (addressed to all tags in the range of a reader) and unicast (addressed to specific tags).

2.1.3 Data Processing Subsystem:

The data processing subsystem is connected to the reader and according to the data the reader receives; it retrieves appropriate information from its own database or external database server [26]. The back-end server has a database and manages various types of information related to each tag, to identify the tag; the tag's response is transmitted securely to it through authenticated reader. This back-end server must be trusted and capable of processing concurrent queries from a lot of readers [26].

A graphical representation of the RFID components and their basic connections is shown next in Figure 2.3.
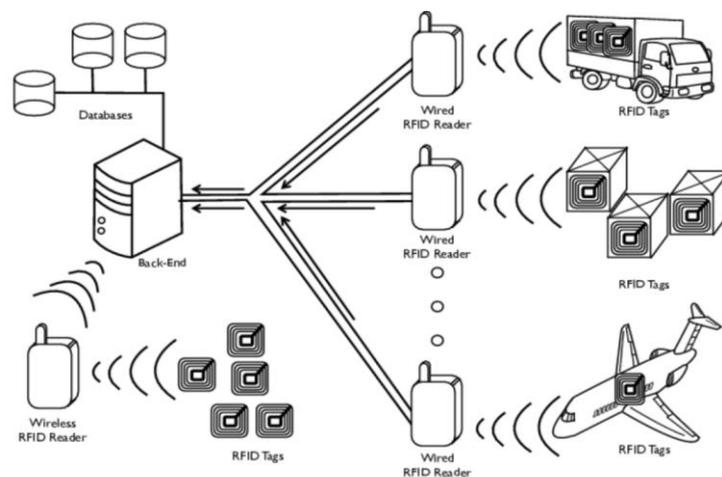
Figure 2.3 Basic components of an RFID system. From left to right: a back-end, RFID readers, and RFID tags [22].

2.2 Benefits of RFID

To demonstrate the potential benefits of RFID, the biggest emphasis is given on comparison with its nearest rival in the market, the optical barcode. The two are different technologies and have different applications, which sometimes overlap, but in many circumstances, RFID offers advantages over traditional barcodes and thus the

growing tendency today is to replace the barcodes with RFID transponders. A direct comparison of the two technologies is provided in the next table.

Table 2.3: RFID vs Barcode: Advantages and disadvantages comparison

	RFID	Barcode
LOS	Not required. Items can have any orientation, as long as it is in the read range.	Definitely required. Scanner must physically see each item directly to scan, and items must be oriented in a very specific manner.
Read Range	Passive UHF RFID: - Up to 40 ft. (fixed readers) - Up to 20 ft. (handheld readers) Active RFID: - Up to 100's of ft. or more	Several inches up to several ft.
Read Rate	High throughput. Multiple (>100) tags can be read simultaneously.	Very low throughput. Tags can only be read manually, one at a time.
Read/Write Capability	More than just reading. Ability to read, write, modify, and update.	Read only. Ability to read items and nothing else.
Human Capital	Virtually none. Once up and running, the system is completely automated.	Very labor intensive; as they must be scanned individually.
Storage Capacity	Large data capabilities such as product maintenance, shipping histories and expiry dates can all	Only the manufacturer and product identification numbers. No additional information such as

	be programmed to the tag.	expiry date etc.
Durability	High. Rugged in nature and much better protected, can even be internally attached, hence operable in very harsh environments.	Low. Easily damaged (ripped) or removed; cannot be read if dirty or greasy.
Security	High. Difficult to replicate. Data can be encrypted; password-protected, or include a "kill" feature to remove data permanently.	Low. Easily reproduced or forged.
Event Triggering	Capable. Can be used to trigger certain events (like door openings, alarms, etc.).	Not capable. Cannot be used to trigger events.
Cost	Expensive. Beside the main cost of the tag's chip, extra cost (and delay) for printing and attaching the tag and the maintenance of databases.	Less expensive. Directly printed onto plastic or paper materials, therefore the only cost involved is the ink; a tiny overall cost.
Technology Maturity	Has global standards, but still an immature technology. Possible standards discrepancies when the tags have to go through different regions of the world.	The most widely used and accepted standard worldwide.

The above comparison shows a clear benefit of RFID over the Barcode technology, with some shortcomings which are currently being worked on throughout the world. After proper weighing of the pros and cons, RFID holds a bigger promise and hence there is a worldwide rush for the development of this technology.

2.3 Application Areas of RFID

Nowadays, due to its flexibility and numerous advantages compared to other identification systems, as discussed in the previous section, RFID is being researched and investigated by both industry and academic scientists and engineers around the world. A significant advancement on this technology has been gained within a short period of time that they are projected now to be implemented in almost all sectors of businesses and service industries. Current diversified RFID applications can be classified into several categories as follows [27] [28]:

1. Supply Chain Management. Some companies have applied RFID technology to track inventories inside their factory and control the overall manufacturing process. With the implementation of RFID into supply chain management came the automation of supply chain management operations and protocols, leading to reduction of annual profit losses due to human error (manually scanning goods) and running out of stocks in retail outlets (RFID enables early detection of depleted goods and resources). Similar tracking scenarios can be applied for libraries, bookstores, airline baggage and livestock.

2. Healthcare. The healthcare industry has been massively investing in RFID to monitor many critical processes, including the healthcare supply chain, prevention of drug counterfeiting and patient safety to name a few. This could reduce the risk of patients' exposure to infected not properly-tracked equipment and assure the un-reusability of discarded drug packaging by companies attempting to sell counterfeit pharmaceuticals.

3. People Management. Some companies and educational institutes have added RFID technology to their systems for managing their members. For example, RFID technology is commonly used to manage employee attendance; and control buildings' access. Many countries have also started using RFID-embedded passports (known as biometric or e-passports) with smart chips that additionally to the traditional passport information: holder's name, date of birth, and other biographic information, contains a biometric identifier.

4. Transportation. Many countries in the world have started using a cashless or 'cash-lite' payment system for public transport by introducing RFID cards that could be loaded in advance with cash. This cashless ticketing decreases the bus drivers' workload and the risk of a traffic accident due to distractions, and ensures accountability and safety in the transport sector by removing the need for commuters to carry cash. Additionally, with proper records of the collected money, the government would be able to tax the income earned from public transport more efficiently.

5. Automatic Payment Method in Stores. At present, a barcode technology is used in many stores for identifying purchased items one by one. By using

RFID, people just need to pass an RFID reader and the payment for all the items will be automatically charged online without waiting at the counter.

Although RFID applications are utilized in many areas, no single RFID system can meet the criteria for all applications because of their different required features. For example, some applications require short range (up to 1.5 m) low cost tags (luggage tagging) while others require long range (over 20 m) and more robust tags (expensive equipment and vehicle tagging). Hence, the design of an RFID system or the picking of an existing one is firmly determined by the application for which it will be used.

Chapter 3

Fading Channels and Backscatter MIMO RFID Systems

3.1 Multipath Fading

Accurate tag reads are vital for the successful implementation of an RFID system. Read reliability of RFID systems is affected by several factors, including multipath fading.

To understand the multipath fading scenario, consider a wave sent from a transmitting antenna. If the transmitting or receiving antenna is close to conducting or dielectric objects, some of the transmitted signal gets scattered off these objects [29].

These scattered waves can reach the receiving antenna by different paths and, as a result, arrive distorted in amplitude, phase and with different angles of arrival. As these waves combine constructively and destructively, the RF tag's received power will vary as a function of its position, a phenomenon known as *multipath fading* and at any given point in space, the RFID system may not have sufficient power to operate properly [29].

A common method to analyze multipath fading is to represent the variation of the received signal strength by a stochastic model. In this approach, the behavior of the signal amplitude—or *envelope* is modeled as a random variable whose value is determined by a prescribed probability distribution function (PDF). Depending on the

nature of the radio propagation environment, there are different models describing the statistical behavior of the multipath fading envelope [30]

3.1.1 Statistical Channel Models of RFID Systems:

The proper characterization of fading PDFs is important for estimating the performance of the RFID system. Therefore, a deep understanding of multipath fading statistics in the backscatter channel is imperative.

Many RFID studies, including the analytical study in [12] [13] [14], and the simulation study in [11] assumed that the RFID subchannels experience non-line-of-sight (NLOS) Rayleigh fading. But since backscatter channels usually exhibit LOS propagation, the Rician fading would be a more appropriate model as stated in [8], [11]. Other studies concluded that the fading gains of the multipath components in an indoor ultrawide bandwidth backscattering channel can be well described by a Nakagami-m distribution [31], [32].

In Chapter 4, the focus will be on the Nakagami-q (Hoyt) distribution, when deriving the mathematical expression for the SER of OSTBC in MIMO RFID backscattering channel. Now, this distribution model is introduced in more details.

3.1.2 Nakagami-q (Hoyt) Distribution:

In communications theory, Nakagami-q (Hoyt) fading is a statistical model used to model signal fading due to strong ionospheric scintillation in satellite communications [17] or in general, those fading conditions more severe than Rayleigh.

This model was first introduced by Nakagami [33] as an approximation for the Nakagami-m fading distribution in the range of fading that extends from the One-sided Gaussian model (when $q = 0$) to the Rayleigh model (when $q = 1$) [34]. Recently, this model is being used more frequently in performance analysis and other studies related to mobile radio communications [17] [18] [19].

If h is defined to be the envelope of a Hoyt fading channel, and Ω is the variance, then the PDF $f_h(h)$ of the random variable h is given by:

$$f_h(h) = \begin{cases} \dfrac{(1+q^2)\,h}{q\Omega}\, e^{-\frac{(1+q^2)^2\,h^2}{4q^2\Omega}} I_0\left(\dfrac{(1-q^4)\,h^2}{4q^2\Omega}\right) & ,\ h \geq 0 \\[2mm] 0 & ,\ h < 0 \end{cases} \tag{3.1}$$

where $I_0(.)$ is the zeroth-order modified Bessel function of the first kind, and q is the Nakagami-q fading parameter [17] . Curves for the PDF of Hoyt distribution for different values of q and Ω are shown in Figure 3.1.
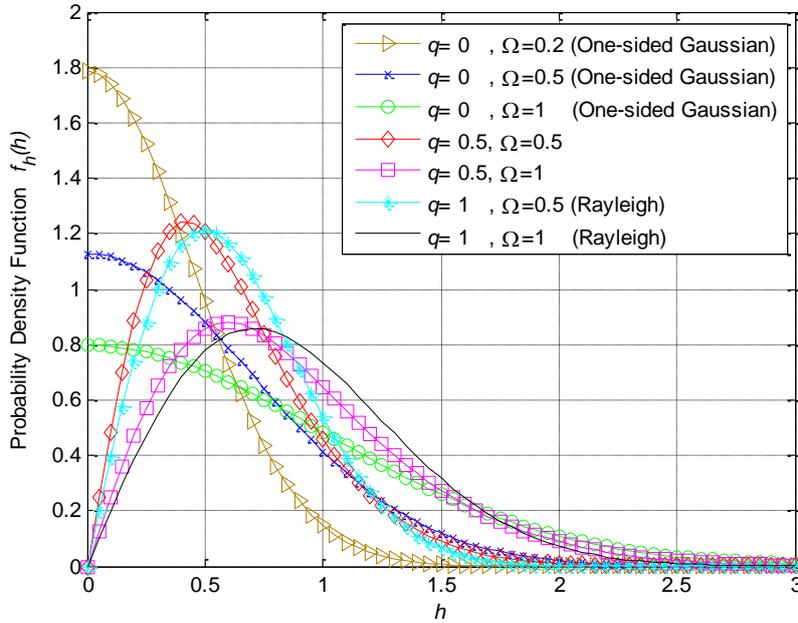
Figure 3.1: Hoyt PDF $\boldsymbol{f_h(h)}$ vs. fading gain $\boldsymbol{h}$ for different values of $\boldsymbol{q}$ and Ω

3.2 Motivation for MIMO RFID

The previous section states that small-scale multipath fading can significantly reduce an RF-tag's read range and reliability. An efficient way to cope with this fading problem is through the use of diversity techniques in which the receiver is afforded multiple, redundant replicas of the transmitted signal under varying fading conditions. These techniques reduce the probability of a deep fade occurring simultaneously to all the signal's replicas [35].

There are several different types of diversity which are commonly employed in wireless communication systems [35]:

- Temporal diversity, in which channel coding and interleaving are used to replicate and distribute the signal in time.

- Frequency diversity, in which the signal is transmitted using several frequency channels or spread over a wide spectrum that is affected by frequency-selective fading.

- Antenna/spatial diversity, in which multiple antennas at the transmitting and/or the reception side are used to provide different copies of the signal that undergo independent fading.

In this thesis, the main focus will be on spatial (antenna) diversity techniques. One way of exploiting antenna diversity is to equip a communication system with multiple antennas at the receiver. This technique is referred to as *receive diversity* and it usually leads to considerable performance gain, both in terms of the interference tolerance and the link budget (which quantifies the link performance by accounting

for all of the gains and losses from the transmitter to the receiver in a system) [36]. The receiver can use one of three diversity combining techniques to improve the quality of the received signal [35]:

- Selection: select the strongest signal from the different signal replicas.

- Switching: switch to another signal when the currently selected signal drops below a predefined threshold.

- Maximal Ratio Combining (MRC): linearly combine a weighted replica of all received signals.

Recently, transmit diversity (equipping the transmitter with multiple antennas) has attracted much attention because of its ability to reproduce many of the benefits as well as a substantial amount of performance gain of receive diversity using new powerful techniques [36]. The next chapter sheds the light on OSTBC the most attractive technique of them.

Schemes which use multiple transmit and receive antennas for communicating over a wireless channel are called MIMO schemes, thus employing multiple antennas at both the RF-reader and the RF-tag results in a RFID-MIMO system.

There have been several studies about RFID-MIMO. Ingram *et al.* [37] were the first to discuss using antenna diversity to mitigate small-scale fading in RFID systems. However, in many later studies equipping the reader with multiple antennas was not purely motivated by small–scale multipath fading. For example, the multi-antenna reader in [38] was used to reduce collisions between simultaneous responses of

multiple proximity tags, where in [39] it was used to improve the localization of RF tags and in [40] to track moving RFID tagged items through its portal.

Others have also proposed using multi-antenna RF tag. But these antennas were not purposely used to combat small-scale multipath fading. For example; in [41] multiple energy-harvesting antennas were used to increase the energy or power/area ratio available to the tag, and in [42] an array of retrodirective antennas permitted the tag to directly point the backscattered signal towards the reader.

In general, it can be concluded that applying multiple transmit and receive antennas (MIMO) setting to the RFID system is an effective approach for solving the NLOS problem when exists, and improving the coverage and the reliability of the system and thus further extending its information-carrying capacity. Additionally, some advanced technology in MIMO can be used to solve the problem of simultaneously detecting several objects.

3.3 Backscatter MIMO RFID Systems

3.3.1 Far-Field Propagation and Backscatter Principle:

Passive tags are the most prominent type in use within RFID today. In general, they are the longest-living, the cheapest, and the easiest to manufacture. Since they do not have an active transmitter that communicates with the interrogator, they typically use a process known as electromagnetic *coupling* to obtain power and transfer data. As shown in Figure 3.2, the main RFID coupling techniques are: the inductive coupling to the reactive energy circulating around the reader antenna and the backscatter (also

known as *radiative*) coupling to the real power contained in free space propagating electromagnetic plane waves [43].
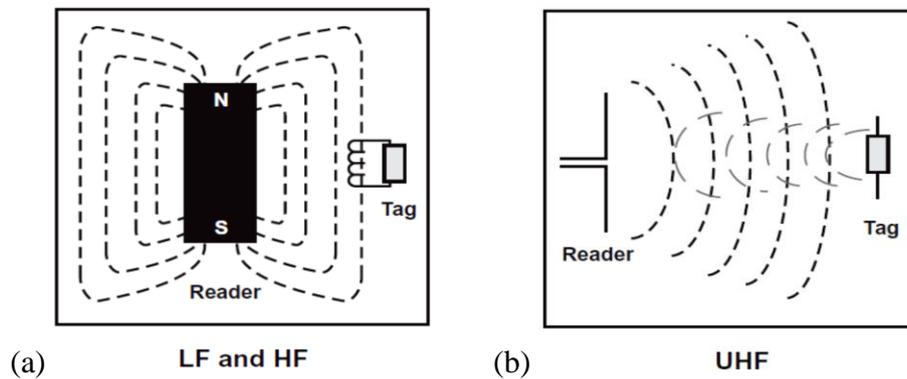
Figure 3.2: The main RFID coupling techniques [44]. (a) Inductive Coupling. (b) Backscatter Coupling.

The type of coupling used depends on the operating frequency and the distance between the tag and the interrogator antenna. Inductive coupling is limited to LF and HF tags with relatively short reading ranges in the near-field zone of the reader, whereas UHF and microwave tags use far-field backscatter coupling to communicate over longer read distances [43].

In this thesis, the term "RF tag" will refer to passive backscatter tags operating in the far-field of the reader, unless specified otherwise. A very simple way to illustrate the operation of a passive backscatter RFID system is shown schematically in Figure 3.3.

The RFID reader transmitter initiates an inventory round by broadcasting an unmodulated carrier or continuous wave (CW), which is also called query signal, the RF tag then responds to this enquiry by backscattering the reader's CW signal. The backscattering (i.e., the reflection of the incoming carrier power) is achieved through

the tag built-in IC which, depending on the data to be transmitted to the reader (i.e. the ID of the tag), switches between different loads and thus controls the reflection coefficient of the tag antenna $\Delta(t)$ and the reflected electromagnetic wave [45].
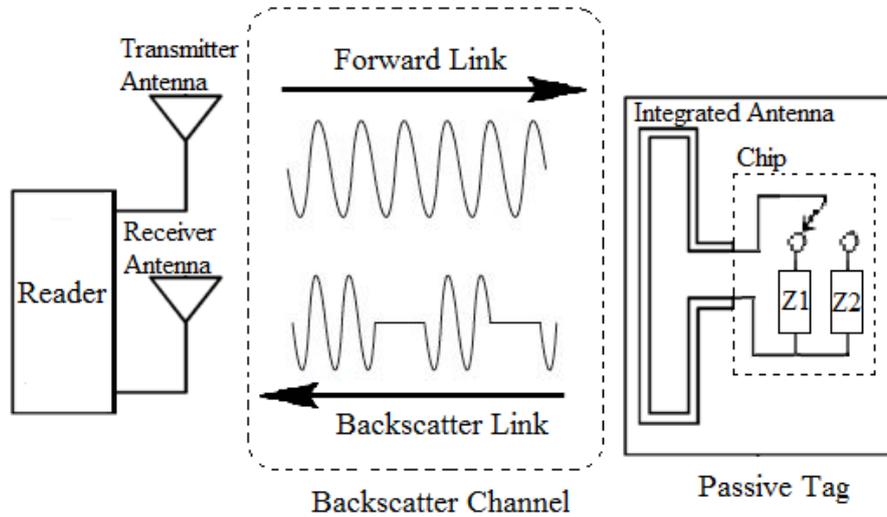
Figure 3.3: The operation of passive backscatter RFID system

3.3.2 The General Mathematical Model of MIMO Backscatter RFID Channel:

The MIMO passive channel was first described in [11], as an $M \times L \times N$ dyadic backscatter channel, that represents the propagation of signals in a backscatter radio system consisting of M transmitter, L RFID tag, and N receiver antennas, shown in Figure 3.4 [13].
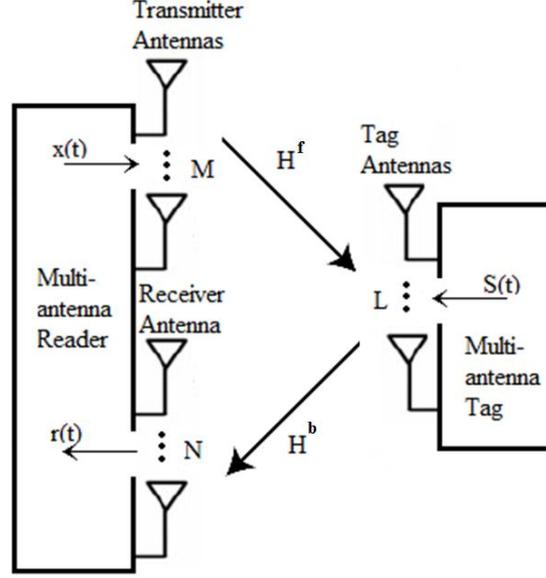
Figure 3.4: The general $M \times L \times N$ dyadic backscatter channel

The received signal from the $M \times L \times N$ dyadic channel (an $N \times 1$ vector) is given by

$$r(t) = H^b S(t) H^f x(t) + n(t) \tag{3.2}$$

where $x(t)$ (an $M \times 1$ vector) is the unmodulated signals transmitted from the reader, $n(t)$ (an $N \times 1$ vector) is the corresponding noises at the reader receivers, H^f (an $L \times M$ matrix) is the channel matrix from the reader to the tag, H^b (an $N \times L$ matrix) is the channel matrix from the tag to the reader and $S(t)$ (an $L \times L$ matrix) is the signalling (also known as *backscattering*) matrix that describes the time-varying modulation and coding of the carrier signals by the L-antenna RF tag [46].

The form of signaling matrix is determined by the physical implementation of the modulation circuitry and RF-tag antennas as follows [29];

- *Identity Signaling Matrix:* when each tag antenna is used to modulate backscatter with the same signal and no signals are transferred between the antennas.

$$\boldsymbol{S_I}(t) = \Delta(t)\,\boldsymbol{I_L} \qquad (3.3)$$

where $\boldsymbol{I_L}$ is the $L \times L$ identity matrix and $\Delta(t)$ is the complex RF-tag antenna reflection coefficient.

- *Diagonal Signaling Matrix:* when the tag antennas modulate backscatter with different signals and no signals are transferred between the antennas.

$$\boldsymbol{S_D}(t) = \begin{bmatrix} \Delta_1(t) & 0 & \cdots & 0 \\ 0 & \Delta_2(t) & \cdots & 0 \\ \vdots & \vdots & \ddots & \vdots \\ 0 & 0 & \cdots & \Delta_L(t) \end{bmatrix} \qquad (3.4)$$

where $\Delta_l(t)$ means the load reflection coefficient of the lth tag antenna.

- *Full Signaling Matrix:* If the tag antennas modulate backscatter independently and signals are transferred between the antennas

$$\boldsymbol{S_F}(t) = \begin{pmatrix} \Delta_1(t) & s_{12}(t) & \cdots & s_{1L}(t) \\ s_{21}(t) & \Delta_2(t) & \cdots & s_{2L}(t) \\ \vdots & \vdots & \ddots & \vdots \\ s_{L1}(t) & s_{L2}(t) & \cdots & \Delta_L(t) \end{pmatrix} \qquad (3.5)$$

where again $\Delta_l(t)$ represent the load reflection coefficient of the lth tag antenna and the off-diagonal elements (i.e., $s_{ij}(t)$ where $i \neq j$) represent the signal transfer between antennas.

25

In this thesis, considering the fact that the reader-transmitting antennas only act as charging devices that send identical query signal from all the M antennas (uniform query scheme) and that the forward channel gains are independent Gaussian, if the total transmitted energy is normalized to unity, the forward channel statistics will be same for any M. So from this time on, the focus will only be on the $1 \times L \times N$ channel and it will be called the $N \times L$ channel for simplicity.

For our passive RFID system, the focus will be on the case where the tag antennas modulate backscatter with different signals and none of the (modulated) backscattered signals are transferred between these antennas, thus our signalling matrix takes the diagonal form in (3.4). This matrix unequal coefficients' can be pre-designed according to a certain space-time code to exploit its remarkable benefits in such systems as explained in the following chapter.

Now, let $\boldsymbol{s} = (\Delta_1(t), \dots, \Delta_L(t))^T$ denote the L transmission symbols simultaneously transmitted from L tag antennas, (the time index t in the model is ignored from now on), as an alternative to (3.2) the received signal vector at a particular time point can be expressed as [46]:

$$\boldsymbol{r} = \boldsymbol{Hs} + \boldsymbol{n} \tag{3.6}$$

where $\boldsymbol{H}$ (an $N \times L$ matrix) is the channel matrix of the $N \times L$ channel, and can be expressed as

$$\boldsymbol{H} = \begin{bmatrix} h_1^f h_{1,1}^b & h_2^f h_{2,1}^b & \dots & h_L^f h_{L,1}^b \\ \vdots & \ddots & \ddots & \vdots \\ h_1^f h_{1,N}^b & h_2^f h_{2,N}^b & \dots & h_L^f h_{L,N}^b \end{bmatrix} \tag{3.7}$$

26

Where h_l^f's $(l = 1, ..., L)$ represent forward channels of the $N \times L$ channel, $h_{l,n}^b$'s $(l = 1, ..., L), (n = 1, ..., N)$ represent backscattering channels and h_l^f and $h_{l,n}^b$ are assumed to be statistically independent of each other [13]. And each element of $\mathbf{n} = (n_1, ..., n_N)^T$ is complex gaussian distributed with zero mean and unit variance. Subchannels h_l^f and $h_{l,n}^b$ follow certain fading distribution depending on the propagation environment.

Chapter 4

Backscatter RFID Systems with Space-time Coding over Hoyt

4.1 A Space-Time Coding Approach for RFID MIMO Systems

The focus of this section is on one of the MIMO transmit schemes, space-time signaling; with a brief overview of employing this technique at the tag end of MIMO RFID systems.

4.1.1 Space-Time Coding:

A space–time code is a family of diversity techniques employed to improve the reliability of data transmission in wireless communication systems using multiple transmit antennas and appropriate signal processing in the receiver [47]. STC relies basically on the diversity concept of providing multiple uncorrelated copies of a signal – *diversity branches*- in the hope that combining these different (hopefully independent) branches will significantly reduce the signal fades and allow reliable decoding.

In the case of Space–Time Block Codes (STBCs) in particular, the data stream to be transmitted is encoded in blocks, and distributed among spaced antennas and across time, which gives the name, "space-time coding". The encoder is simply represented by a matrix; each row denotes a time slot while each column represents one antenna's transmissions over time.

$$\mathcal{G} = \begin{bmatrix} z_{11} & z & \cdots & z_{1L} \\ z_{21} & z_{22} & \cdots & z_{1L} \\ \vdots & \vdots & & \vdots \\ z_{T1} & z_{T2} & \cdots & z_{TL} \end{bmatrix} \tag{4.1}$$

where, z_{ij} is the modulated symbol to be transmitted in time slot i from antenna j. There are to be T time slots and L transmit antennas as well as N receive antennas. Defining the code rate as the average number of transmitted symbols per time slot over the course of one block, then if this block encodes k symbols, the code-rate is $c = k/T$ [48].

To provide an elegant encoding and linear decoding technique while offering full diversity benefits in MIMO environments, the STBC is designed to be orthogonal; columns of its coding matrix are pairwise-orthogonal. The main drawback of STBC is that full-rate codewords exist only for up to four antennas, if real signaling is employed and for up to two antennas, if complex signal constellations are used [49]. This rate limitation can be overcome by quasi-orthogonal STBCs that sacrifice the orthogonality of the code at the expense of inter-symbol interference (ISI) [50] .

Before proceeding to employing STBCs in RFID, it is worthwhile now to briefly introduce the Alamouti code and its generalized version (OSTBC).

4.1.1.1 Alamouti Scheme:

Alamouti proposed the simplest and most attractive of all the STBCs in 1998 [51] , it was designed for a two-transmit antenna system and has the coding matrix:

$$\mathcal{G}_2 = \begin{bmatrix} z_1 & z_2 \\ -z_2^* & z_1^* \end{bmatrix} \tag{4.2}$$

where * denotes complex conjugate.

During the first symbol period, z_1 and z_2 will be transmitted from antennas 1 and 2 respectively. During the second symbol period, $-z_2^*$ and z_1^* will be transmitted from antennas 1 and 2 respectively. Since two information symbols are transmitted over two time intervals, this code achieves full rate.

It is the only orthogonal STBC that, for complex modulation symbols, achieves rate-1 without needing to sacrifice its data rate. Since almost all constellation diagrams rely on complex numbers, Alamouti's code has a significant advantage over the higher-order STBCs despite their better error-rate performance.

4.1.1.2 Higher order Orthogonal Space-Time Block Codes (OSTBCs):

Tarokh *et al*. [52] extended the Alamouti scheme to a general case; called OSTBC with an arbitrary number of transmit antennas.

These codes retain the property of having linear maximum-likelihood decoding with full transmit diversity at low computational cost but they have little or no coding gain. To provide both diversity and coding gain, one can choose a space-time code that has an in-built channel coding mechanism, for example space-time trellis codes.

4.1.2 Employing Space-Time Codes in RFID Systems:

Space-Time codes are employable in passive RFID systems whenever the tag is equipped with multiple antennas. Information is encoded across the multiple tag antennas and received by the reader, which also typically possesses multiple antennas. In [6], the authors first proposed to apply the Alamouti space-time coding technique to the RFID systems, they presented a closed-form expression for the BER of the RFID system with the noncoherent frequency shift keying modulation and multiple transmit antennas at the tag and single transmit/receive antenna at the reader, where Rayleigh distributed forward and backscattering links are assumed.

A number of later MIMO RFID studies have also applied this technique but with some variations on the environment. For example: the authors in [13] analyzed the BER performance of the MIMO RFID channel under two transmission schemes, the identical signaling transmission scheme and the Alamouti's coding scheme, but with binary phase shift keying (BPSK) modulation and multiple reader receive antennas. While [16] differs only by assuming Nakagami-m and Rician fading distributions at the forward and backward links.

Similar to the aforementioned studies, a note was made in the previous chapter of using tag antennas with unequal reflection coefficients and with no signal transfer between them in our customized MIMO RFID model. And that this diagonal signaling matrix can be obtained by pre-designing the coefficients according to a certain space-time code.

Thus, if Alamouti's code is to be implemented, the tag circuit design will follow the diagonal signaling matrix at time slots t = 1 and t = 2 as

$$S_D(1) = \begin{bmatrix} z_1 & 0 \\ 0 & z_2 \end{bmatrix}, S_D(2) = \begin{bmatrix} -z_2^* & 0 \\ 0 & z_1^* \end{bmatrix} \qquad (4.3)$$

If a tag with two antennas carries the ID $(z_1; z_2; z_3; z_4)$ for example, one way to implement the signaling scheme of (3.4) is to design the reflection coefficients of one antenna loading to be $(z_1; -z_2^*; z_3; -z_4^*)$, and the coefficients of the other antenna loading to be $(z_2; z_1^*; z_3; z_4^*)$.

4.2 A Conditional MGF Approach for OSTBCs

The PDF approach is a widely used approach to evaluate the SER performance of different wireless channels, it's based on evaluating the distribution associated with the channel matrix first [53]. For the RF backscattering channel case because of its complex query-fading-coding-fading structure, applying this approach is not preferable. Alternatively, [16] proposed the conditional MGF approach, as described next.

We assume that the channel is a quasi-static fading channel and the channel state information is known at the reader. Because of its orthogonality property, OSTBC can be transformed from the MIMO fading channel in (3.6) to the following Q parallel single-input–single-output (SISO) channels [54] :

$$\acute{r} = \sqrt{||H||_F^2}\, \acute{s} + w \qquad (4.4)$$

where $\acute{r} = (\acute{r}, \dots, \acute{r}_Q)^T$ represents the received symbols that can be detected based on a simple maximum-likelihood method, $||\boldsymbol{H}||_F = \sqrt{\sum_{n=1}^{N} \sum_{l=1}^{L} |h_l^f h_{l,n}^b|^2}$ is the Frobenius norm of $\boldsymbol{H}$, $\acute{s} = (\acute{s}_1, \dots, \acute{s}_Q)^T$ represents the Q incoming symbols, and each element of $\boldsymbol{w} = (w_1, \dots, w_Q)^T$ is complex gaussian distributed with zero mean and unit variance.

Let E_b denote the average energy per bit and E_s denote the average energy per symbol, then $E_s = E_b \log_2 K$ where K is the size of the signal constellation. The instantaneous signal-to-noise ratio (SNR) per symbol is therefore given by $\gamma = \frac{||H||_F^2 \log_2 K}{R} \frac{E_b}{N_0} = \frac{||H||_F^2 \log_2 K}{R} \bar{\gamma} = ||H||_F^2 \, g \, \bar{\gamma}$, where $R = \frac{M}{T}$ is the symbol rate, M is the total number of distinct symbols, T is the symbol duration time and $g = \frac{\log_2 K}{R}$.

The SER of OSTBC can be calculated by averaging the density of $||H||_F^2$ over

$$Q\left(\sqrt{g\bar{\gamma} \, ||\boldsymbol{H}||_F^2}\right)$$

$$P_{OSTBC}(\bar{\gamma}) = E_H\left(Q\left(\sqrt{g\bar{\gamma}||H||_F^2}\right)\right) = \frac{1}{\pi} \int_{\theta=0}^{\pi/2} G(\bar{\bar{\gamma}}) \, d\theta \qquad (4.5)$$

Here, the alternative representation of the gaussian Q function as in [53] is employed, where $Q(x) = \frac{1}{\pi} \int_{\theta=0}^{\pi/2} exp(-\frac{x^2}{2sin^2\theta}) \, d\theta$ for $x \geq 0$, $\bar{\bar{\gamma}} = \frac{g\bar{\gamma}}{sin^2\theta}$ and $G(\bar{\bar{\gamma}}) = E_H\left(\exp\left(-\frac{g\bar{\gamma}||H||_F^2}{sin^2\theta}\right)\right)$ is the MGF of $||H||_F^2$.

To find $G(\bar{\bar{\gamma}})$, define

$$\left|\left|\boldsymbol{H}\right|\right|_F^2 = \sum_{l=1}^{L}\left|\left|\boldsymbol{H}_l\right|\right|_F^2 = \sum_{l=1}^{L}\sum_{n=1}^{N}\alpha_l\beta_{l,n} \qquad (4.6)$$

where $\left|\left|\boldsymbol{H}_l\right|\right|_F^2$ is the squared Frobenius norm of the lth column of H, $\alpha_l = |h_l^f|^2$ and $\beta_{l,n} = |h_{l,n}^b|^2$. One can see that $\left|\left|\boldsymbol{H}_l\right|\right|_F^2$'s are independent random variables; therefore, the MGF $G(\bar{\bar{\gamma}})$ can be represented as a multiplication of the MGFs of $\left|\left|\boldsymbol{H}_l\right|\right|_F^2$'s

$$G(\bar{\bar{\gamma}}) = \prod_{l=1}^{L}G_l(\bar{\bar{\gamma}}) \qquad (4.7)$$

If α_l is fixed, the random variable $\left|\left|\boldsymbol{H}_l\right|\right|_F^2 = \alpha_l\sum_{n=1}^{N}\beta_{l,n}$ is exactly the same as the gain of an N-branch single-input multiple-output system with MRC at the receiver, with N branches $h_{l,n}^b = \alpha_l\beta_{l,n}$ for $n = 1,\ldots,N$, and each branch has transmission power α_l.

Therefore, the MGF $G_l(\bar{\bar{\gamma}})$ is

$$G_l(\bar{\bar{\gamma}}) = \int_0^\infty \prod_{n=1}^{N}G_{h_{l,n|\alpha_l}}(\bar{\bar{\gamma}})\ f_{\alpha_l}(\alpha_l)d\alpha_l \qquad (4.8)$$

Therefore,

$$G(\bar{\bar{\gamma}}) = \prod_{l=1}^{L}\left(\int_0^\infty \prod_{n=1}^{N}G_{h_{l,n|\alpha_l}}(\bar{\bar{\gamma}})\ f_{\alpha_l}(\alpha_l)\ d\alpha_l\right) \qquad (4.9)$$

where $f_{\alpha_l}(\alpha_l)$ is the pdf of α_l and $G_{h_{l,n|\alpha_l}}(\bar{\bar{\gamma}})$ is the MGF of conditional distribution of $h_{l,n}$ on α_l (i.e., the squared magnitude of the lth forward channel gain). This formulation is applicable to any sub-channels fading assumptions. Next, it will be employed to find the SER performance under Hoyt fading.

4.3 A Conditional MGF Approach for OSTBCs over Hoyt

As noted before the result found in equation (4.9) is general for any fading distribution assumption. In [16] the SER performance of OSTBC of MIMO RFID system is evaluated over the Rician and Nakagami-m fading distribution. Here, the performance of the OSTBC for MIMO RFID channels is revisited to derive a mathematical expression for the SER performance when Hoyt fading distribution is assumed at the forward and backward links.

For Hoyt fading, the pdf of α_l is

$$f_{\alpha_l}(\alpha_l) = \frac{1+q_f^2}{2q_f} e^{\frac{-\left(1+q_f^2\right)^2 \alpha_l}{4\,q_f^2}} I_0\left(\frac{1-q_f^4}{4q_f^2}\,\alpha_l\right) \tag{4.10}$$

where q_f is the q factor of the forward channel. In Hoyt fading, the MGF of $\beta_{l,n} = |h_{l,n}^b|^2$ is given by [53]

$$G_{\beta_{l,n}}(\bar{\bar{\gamma}}) = \left(1 + 2\bar{\bar{\gamma}} + \frac{q_b^2\,(2\bar{\bar{\gamma}})^2}{(1+q_b^2)^2}\right)^{\frac{-1}{2}} \tag{4.11}$$

Therefore, the conditional MGF $G_{h_{l,n|\alpha}}(\bar{\bar{\gamma}})$ can be given by multiplying the SNR of (4.11) by α_l

$$G_{h_{l,n|\alpha}}(\bar{\bar{\gamma}}) = \left(1 + 2\alpha_l\bar{\bar{\gamma}} + \frac{q_b^2\,(2\alpha_l\bar{\bar{\gamma}})^2}{(1+q_b^2)^2}\right)^{\frac{-1}{2}} \tag{4.12}$$

where q_b is the q factor of the backscattering channel. Substitute $f_{\alpha_l}(\alpha_l)$ and $G_{h_{l,n}|\alpha}(\bar{\bar{\gamma}})$ into (4.8), the exact form of $G_l(\bar{\bar{\gamma}})$ can be given as (see Appendix A)

$G_l(\bar{\bar{\gamma}}) =$

$$\begin{cases} \sum_{m=0}^{\infty} \frac{D_1 D_2^{2m}}{(m!)^2} \frac{(D_1^2)^{-(2m+1)}}{(k_b-1)} \left(k_b \, M\left(\frac{2\,k_b\bar{\bar{\gamma}}}{k_1 D_1^2}, 2m+1,1 \right) - M\left(\frac{2\,\bar{\bar{\gamma}}}{k_1 D_1^2}, 2m+1,1 \right) \right) & ,N=2 \\[2em] \sum_{m=0}^{\infty} \frac{D_1 D_2^{2m}}{(m!)^2} \frac{(D_1^2)^{-(2m+1)}}{(k_b-1)} \left(\begin{array}{l} (k_b-1)M\left(\frac{2\,\bar{\bar{\gamma}}}{k_1 D_1^2}, 2m+1,2 \right) - k_b^2(1-k_b)\,M\left(\frac{2\,k_b\,\bar{\bar{\gamma}}}{k_1 D_1^2}, 2m+1,2 \right) \\ + 2k_b M\left(\frac{2\,\bar{\bar{\gamma}}}{k_1 D_1^2}, 2m+1,1 \right) - 2k_b^2 M\left(\frac{2k_b\bar{\bar{\gamma}}}{k_1 D_1^2}, 2m+1,1 \right) \end{array} \right) & ,N=4 \end{cases}$$

$$(4.13)$$

where $k_f = q_f^2$, $k_b = q_b^2$, $k_1 = 1 + k_b$, $k_2 = 1 + k_f$, $D_1 = \frac{1+k_f}{2\sqrt{k_f}}$, $D_2 = \frac{1-k_f^2}{8\,k_f}$

,and $D_3 = \frac{4\,k_b}{(1+k_b)^2}$. In addition, the function

$M(s, \acute{m}, \acute{N}) = \int_{t=0}^{\infty} t^{\acute{m}-1} e^{-t} (1 + s\,t)^{-\acute{N}} dt$ was well studied in [55] and has a

closed form of

$$M(s, \acute{m}, \acute{N}) \doteq e^{\frac{1}{s}} s^{-\acute{N}} \sum_{k=0}^{\acute{m}-1} \binom{\acute{m}-1}{k} \left(-\frac{1}{s} \right)^{\acute{m}-k-1} \Gamma\left(k - \acute{N} + 1, \frac{1}{s} \right) \qquad (4.14)$$

When exact forms are complicated, asymptotic expressions are often obtained to provide a more comprehensive view. Asymptotically, in high SNR regimes:

$$G_l(\bar{\bar{\gamma}}) \doteq \begin{cases} \frac{C_{1\_2}^f \, C_{2\_2}^b}{g} \, \bar{\bar{\gamma}}^{-1}, & if\ N=2 \\[1.5em] \frac{C_{1\_4}^f \, C_{2\_4}^b}{g} \, \bar{\bar{\gamma}}^{-1}, & if\ N=4 \end{cases} \qquad (4.15)$$

Substituting (4.15) into (4.7) then into (4.6) can yield asymptotic expression of SER for OSTBC (see Appendix A)

$$P_{OSTBC}(\bar{\gamma}, N, L) \doteq \begin{cases} C_L \left(\frac{C_{1\_2}^f \, C_{2\_2}^b}{g} \right)^L \bar{\gamma}^{-L}, & if\ N=2 \\[2em] C_L \left(\frac{C_{1\_4}^f \, C_{2\_4}^b}{g} \right)^L \bar{\gamma}^{-L}, & if\ N=4 \end{cases} \qquad (4.16)$$

where $C_{1\_2}^f = \frac{1+k_f}{2\sqrt{k_f}}$, $C_{2\_2}^b = \frac{k_1 ln(k_b)}{2(k_b-1)}$, $C_{1\_4}^f = \frac{1+k_f}{2\sqrt{k_f}}$, $C_{2\_4}^b = \frac{k_1^2}{2(k_b-1)^2} - \frac{k_b k_1 ln(k_b)}{(k_b-1)^3}$, and

$$C_L = \frac{\Gamma\left(L+\frac{1}{2}\right)}{2\sqrt{\pi}\,\Gamma(L+1)}.$$

For the special case of Rayleigh fading channels, the SER expressions for the MIMO RFID system with space-time coding can be found from (4.16) by setting $(q_f, q_b) =$ (1,1). But since direct substitution of $q_b = 1$ results in indeterminate forms (0/0) for the coefficients of backscatter link, instead, the L'Hôpital's rule is repeatedly used to help evaluate the limit as (q_f, q_b) approaches (1,1), with which (4.16) reduces to

$$P_{OSTBC}(\bar{\gamma}, N, L) \doteq \begin{cases} C_L \left(\frac{1}{g}\right)^L \bar{\gamma}^{-L}, & if\ N = 2 \\ C_L \left(\frac{1}{3g}\right)^L \bar{\gamma}^{-L}, & if\ N = 4 \end{cases} \qquad (4.17)$$

where $\lim_{q_b \to 1} C_{2\_2}^b = \lim_{q_b \to 1} \frac{k_1 ln(k_b)}{2(k_b-1)} = 1$ and

$\lim_{q_b \to 1} C_{2\_4}^b = \lim_{q_b \to 1} \left(\frac{k_1^2}{2(k_b-1)^2} - \frac{k_b k_1 ln(k_b)}{(k_b-1)^3}\right) = \lim_{q_b \to 1} \frac{k_1^2(k_b-1) - 2 k_b k_1 ln(k_b)}{2(k_b-1)^3} = \frac{1}{3}$.

Eq. (4.17) is equivalent to eq. (33) in [13] for the Rayleigh fading when $N = 2, 4$.

Chapter 5

Numerical Results and Discussion

The SER performance of orthogonal space–time block-coded MIMO RFID system in Hoyt fading channel is evaluated and discussed in this chapter. Firstly, the asymptotic and exact SER curves are plotted and compared for different number of tag and reader antennas. Toward this end, the focus was only on the case of coherent BPSK modulation scheme. Then different observations and properties of the system are discussed.

Next, the suitability of modeling a Hoyt-fading environment by a properly chosen Nakagami-m model is assessed, as far as the error performance of the OSTBC over Hoyt backscattering channel is concerned. To furtherly verify the correctness of our derived Hoyt-SER performance expression, few performance comparisons are done with those of the same MIMO RFID system but under different fading distributions that can also be narrowed down to the special case that the Hoyt fading covers. Finally, the chapter is concluded by studying the effect of various modulation schemes on the system performance.

5.1 General Observations

The exact and asymptotic expressions for two and four reader-receiving antennas are analysed. The following set of figures show the SER/BER curves of OSTBC scheme with BPSK modulation in the Hoyt $N \times L$ MIMO RFID channel (the SER and BER are exactly same when using BPSK).
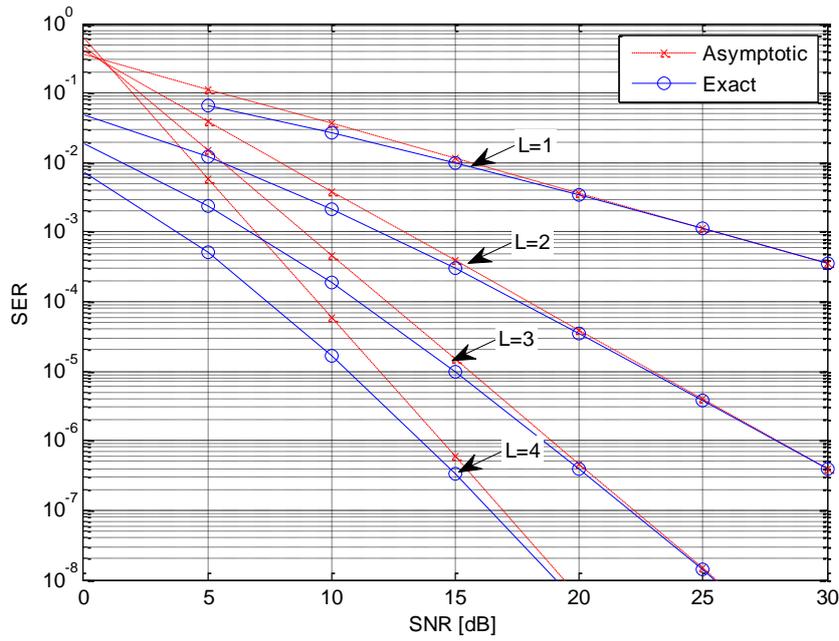
Figure 5.1: SER performances of the RFID channel for different number of tag antennas (L), with $N = 2$ and $q_f = q_b = 0.5$.
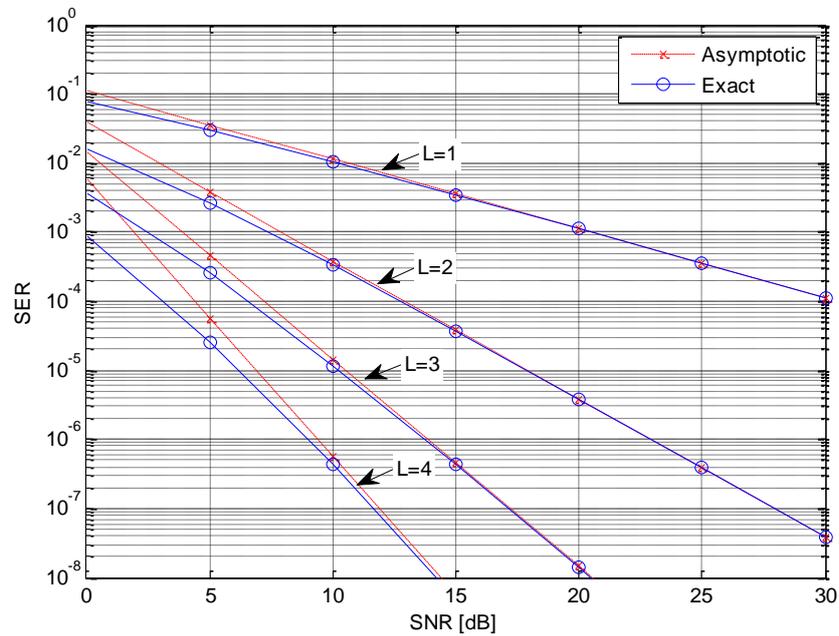
Figure 5.2: SER performances of the RFID channel for different number of tag antennas (L), with $N = 4$ and $q_f = q_b = 0.5$.

For different tag-antennas number, it is observed that our asymptotic results match well with exact expressions for the two cases (*N=2, N=4*) and that the convergence

between the exact and asymptotic SER curves takes place at a high value of SNR, thus validating the correct approximation procedure for the system in high SNR regimes.

5.2 Properties of MIMO RF Backscattering Channel

Next, two important properties for this RFID channel are discussed: the achievable diversity order and the effects of forward and backscattering links on the performance.

5.2.1 Diversity Order:

The diversity order measures how many statically independent copies of the same symbol the receiver is able to separate. When SNR tends to infinity the slope of SER vs. SNR in log-scale shows the diversity order. For the asymptotic expressions in (4.16) the asymptotic diversity orders for the Hoyt fading MIMO RF backscattering channel with ($N=2$, $N=4$) are

$$d_a = \lim_{\overline{\gamma} \to \infty}(-\frac{\log P(\overline{\gamma})}{\log \overline{\gamma}}) = L \qquad (5.1)$$

As also observed in Figure 5.3, where the slopes of these SER curves only depend on L, the receiving antennas N does not affect the diversity order.
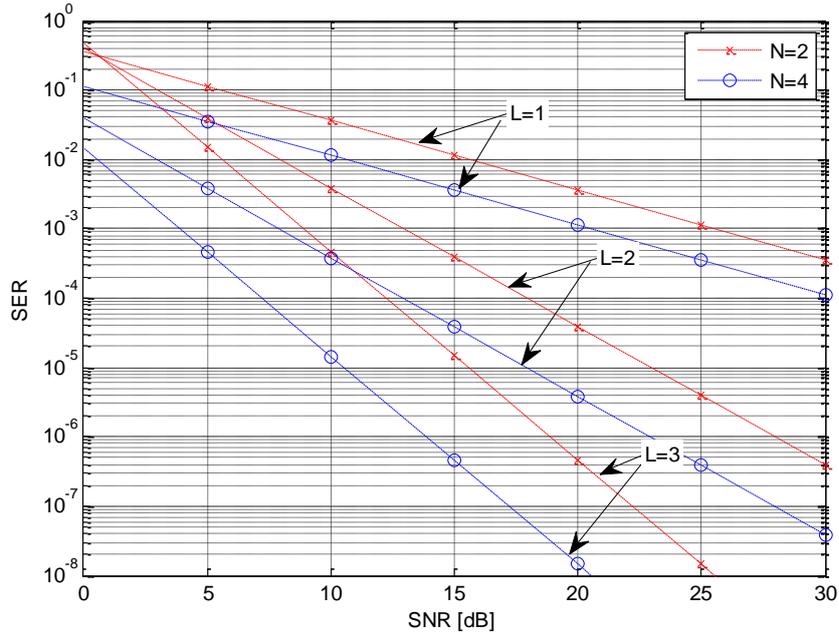
Figure 5.3: The asymptotic diversity orders for the Hoyt fading MIMO RF backscattering, with $q_f = q_b = 0.5$.

Figure 5.3 also illustrates the effect of increasing the number of diversity branches (from $L=1$ to $L=3$ and from $N=2$ to $N=4$) on the SER curves of the RFID system for Hoyt faded signals. It is noticed that the SER is greatly reduced when increasing the number of diversity branches. For example, when $SNR = 15\ dB$ the SER values for $(L, N) = (1,2), (1,4), (2,2), (2,4)$ are $11.5 * 10^{-3}$, $3.56 * 10^{-3}$, $0.436 * 10^{-3}$ and $0.042 * 10^{-3}$ respectively. This means that the more is the diversity branches, the less is the error rate. As mentioned in Chapter 3, diversity techniques are used to combat signal fading, where the probability that all copies of the signal will undergo the same fading is small, thus, the use of diversity schemes at the transmit and/or the receive side will enhance the overall performance of the MIMO RFID system.

5.2.2 Impact of Forward and Backscattering Channel Conditions:

Another appealing property of the MIMO RF backscattering channel is that the channel condition of the forward link has a more noticeable impact on performance than to that of the backscattering link. For example, for Hoyt fading with ($N = 2$), Figure 5.4 implies that, with $q_f = 0.3$ being fixed, changing q_b (0.3, 0.6, and 0.9) doesn't have a notable effect on the SER curves. Contrarily, with $q_b = 0.3$ being fixed, SER curves significantly change when q_f (0.3, 0.6, and 0.9) changes. Figure 5.5 shows that similar observations are true for the Hoyt distributed forward and backscattering links with four reader-receiving antennas.
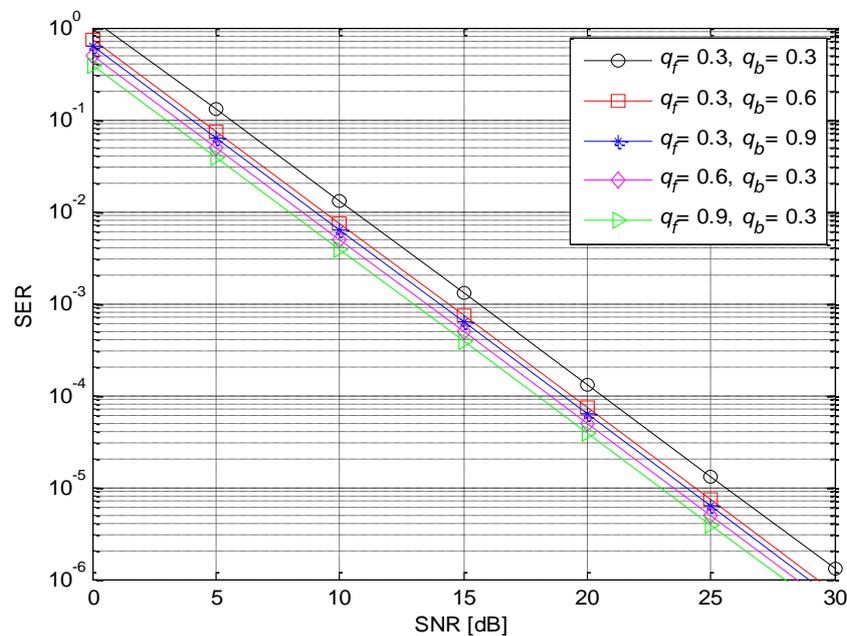
Figure 5.4: The effects of forward and backscatter links on the performance. Here, $N = 2$, $L=2$
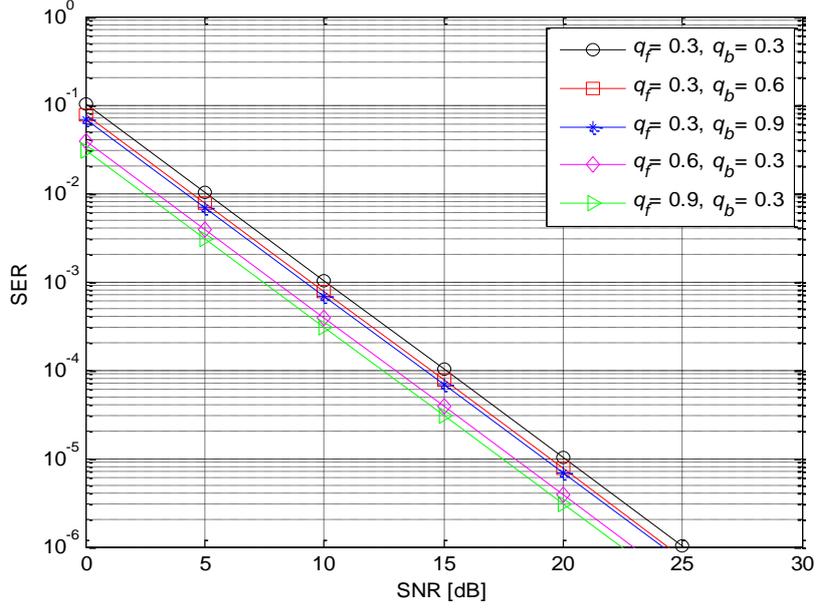
Figure 5.5: The effects of forward and backscatter links on the performance. Here, $N= 4$, $L=2$

A plot of the asymptotic expressions' coefficients in (4.16) will perfectly consists with these findings, where the effect of the forward channel is reflected by coefficients $C_{1\_2}^f$ and $C_{1\_4}^f$, and that of the backscattering channel is reflected by $C_{1\_2}^b$ and $C_{1\_4}^b$ for $N = 2$ and $N = 4$, respectively.
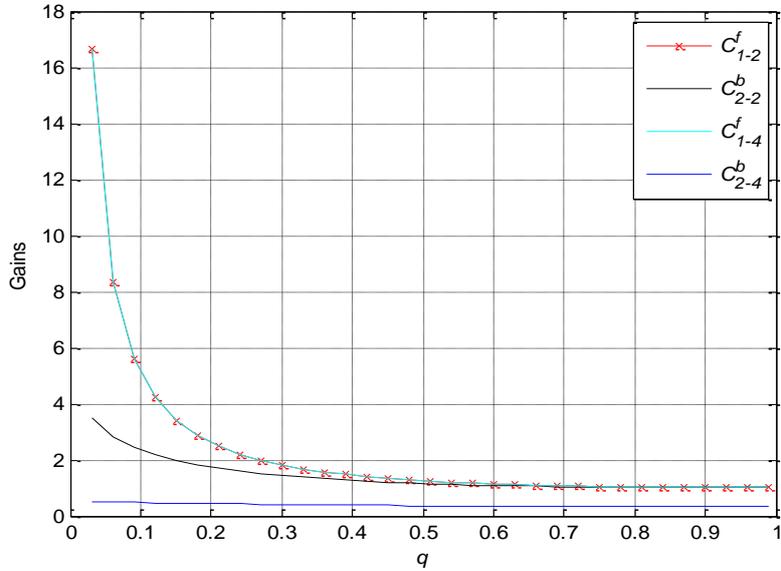
Figure 5.6: The coefficient of backscatter link C^b is almost constant as the q_b increases, whereas the coefficient of forward link C^f significantly decreases as the q_f increases.

In addition, a general conclusion can be extracted with regard to the impact of the fading severity over both the forward and backscattering links, that increasing the value of the shape parameter q (i.e. a less severe fading) results in a better performance of the RFID system as indicated by the decreased SER value.

5.3 Approximation of the Hoyt Model by the Nakagami-m Model

This section examines the suitability of modeling a Hoyt-fading environment by a properly chosen Nakagami-m model, as far as the error performance of the OSTBC model in MIMO RFID system is concerned. The approximation of the Hoyt model by a suitable Nakagami-m model was proposed by Nakagami in [33]. The relation between the fading parameter of the Nakagami-m distribution, m, and the q fading parameter was given by

$$m = \frac{(1+q^2)^2}{2(1+2q^4)} \quad , \ m \leq 1 \tag{5.2}$$

In order to examine the approximation of the Hoyt fading environment by a suitable Nakagami-m model, using (5.2), in Figure 5.7 curves are given for the error performance of RFID-MIMO system for BPSK modulation both in Hoyt and Nakagami-m fading environments. A Nakagami-m model with $m = 0.75$, that approximates a Hoyt fading environment with $q = 0.7$, is used.

The results obtained here show that the equivalence of the two models worsens as the average SNR increases and as the number of branches L decreases. For example, at

SER = 10^{-3} , the Hoyt model is 3.0771, 1.618, 0.8921 dB superior of the equivalent

Nakagami-m model using $L = 2,3,4$, respectively . The corresponding values at SER

= 10^{-4} are 4.748, 2.72, and 1.7314, respectively. For a more severe Hoyt fading

environment with $q = 0.3$, as shown in Figure 5.8, it can be easily shown that for SER

=10^{-3}, the performance of the Hoyt model is 3.719, 0.696, 0.756 dB superior of the

equivalent Nakagami- m model with $m = 0.6944$, for $L = 2,3,4$ respectively, since for

SER = 10^{-4} the corresponding values are 7.197, 2.994, and 0.968 dB, respectively.
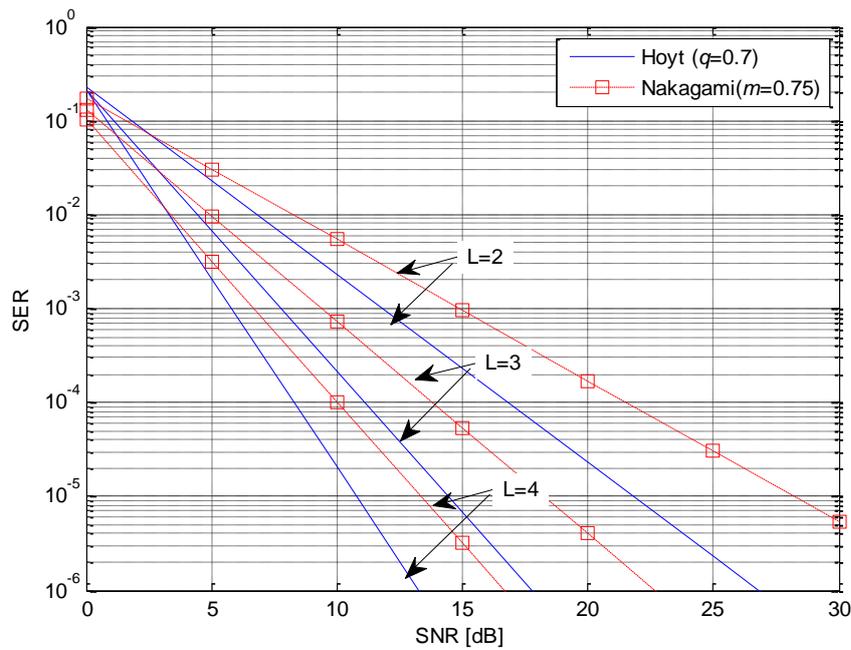
Figure 5.7: Approximation of the error performance in Hoyt fading environment with $q = 0.7$,
with a Nakagami-m model.
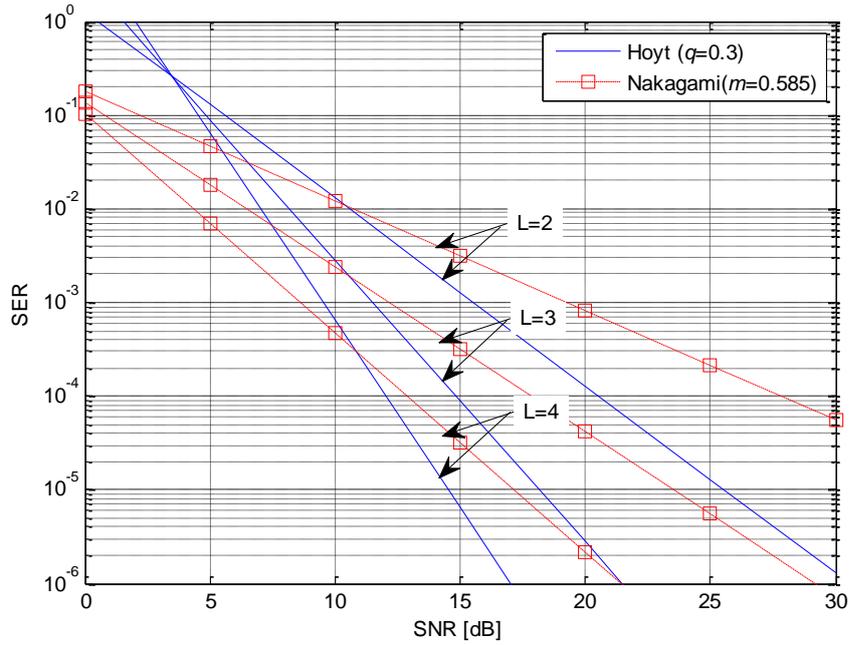
Figure 5.8: Approximation of the error performance in Hoyt fading environment with $q = 0.3$ with a Nakagami-m model.

By comparing the results for the approximations of the two Hoyt fading environments with the equivalent Nakagami-m models, it is observed that the equivalence between the two models improves as the fading gets less severe (i.e as the value of the shape parameter q increases).

The above two figures also show that the approximation of the Hoyt fading environment with the equivalent Nakagami-m model, as suggested by (5.2), always underestimates the performance of the Hoyt model (gives an upper bound). The same result was obtained in [18] while studying the performance of predetection EGC receivers over Rice- and Hoyt-fading channels. Thus, we can't rely on the approximation relation between the two models to directly obtain the Hoyt case curves from the Nakagami$-m$ SER expressions derived in previous studies, especially for severe fading cases. This motivates the need for separately deriving the Hoyt SER performances expressions.

5.4 Special Case

Nakagami distributions, namely Nakagami-q (Hoyt), Nakagami-m and Nakagami-n (Rician), cover the Rayleigh fading distribution model as a special case when $q = 1$, $m = 1$ and $n = 0$, respectively.

In [13] the authors studied the SER performance of MIMO RFID system assuming a Rayleigh fading channel, where in [16] the SER performances under Rician fading and Nakagami-m fading were studied. In the previous chapter, the focus was on the SER performance under Hoyt fading and reducing its SER expressions to the same Rayleigh expressions in [13] when $q \rightarrow 1$.

To furtherly validate our newly-derived results, in Figure 5.9 the expressions derived in the all the above studies are used, and by setting the parameters of each distribution to represent the Rayleigh case, it was found that our curves are comparable with theirs and the achievable performance when $q \rightarrow 1$ is practically coincident with the Rayleigh case obtained from all other distributions.
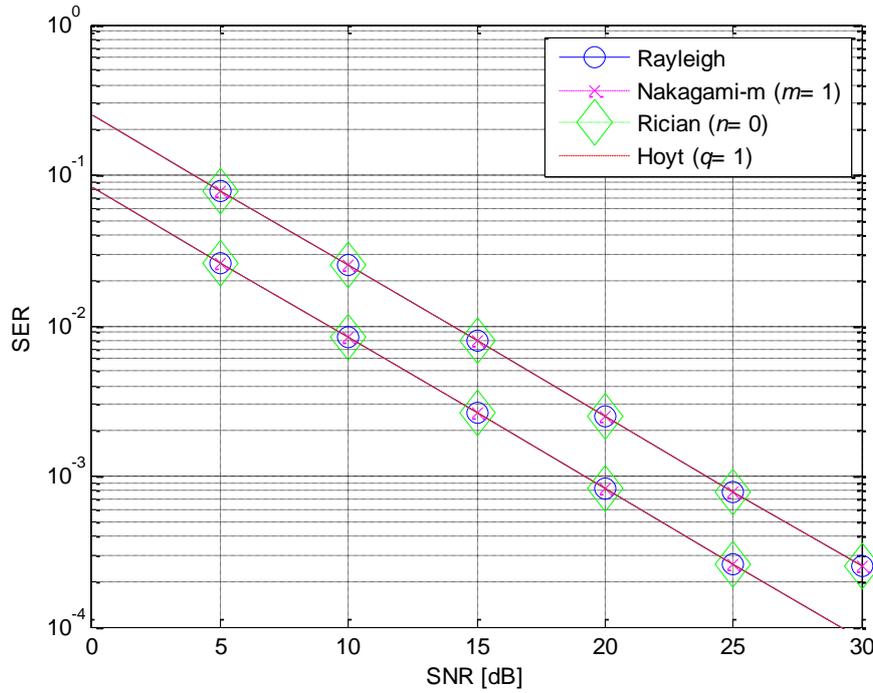
Figure 5.9: SER performances of the RFID channel over Rayleigh fading channel using SER expressions of different fading models, with $(L = 1, N = 2,4)$, from the top to the bottom

5.5 Modulation Schemes

The asymptotic expressions of SER for OSTBC in (4.16) are applicable for different modulation schemes. By setting the appropriate value of the constant $g = \frac{\log_2 K}{R}$, different schemes can be obtained, for example $g = 1$: coherent binary phase-shift keying (BPSK), $g = 0.5$: coherent binary frequency-shift keying (BFSK) , $g = 0.25$: coherent amplitude-shift keying (ASK) [53].

The SER for OSTBC combined with three types of modulation format is shown in Figure 5.10. The tag ID is encoded using a space–time block code, and the

constellation symbols are transmitted from different antennas. The results are presented for two tag antennas with two reader receiving antennas.
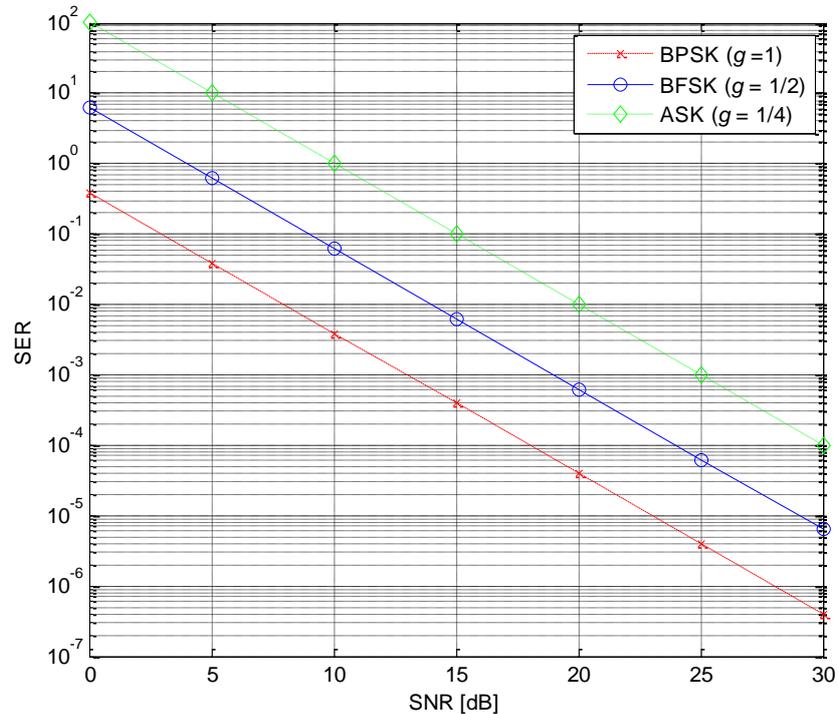
Figure 5.10: SER performances of the RFID channel over a Hoyt fading channel under different modulation scheme for two transmit and two receive antenna. Here $q_f = q_b = 0.5$.

The SER performance of the STBC over Hoyt fading channel shows that the BPSK gives a better performance than the BFSK and ASK modulation schemes.

For example, it is observed that for $N = 2$ at the SER of 10^{-2}, the code with BPSK and is superior by about 5.867 dB and 11.582 dB to the codes with BFSK and ASK, respectively. It can be concluded that the BFSK and ASK modulation schemes, need better channel conditions than the BPSK modulation scheme for a given SER criteria.

Chapter 6

Conclusion and Future Work

6.1 Conclusion

In this thesis, the light was shed on "Radio Frequency Identification (RFID)" as an emerging contactless automatic identification technology that is tracking consumer products worldwide. A mathematical modelling of the MIMO backscatter RFID channel was provided and many challenges were observed that it poses due to its querying-fading-signalling-fading structure.

Using STBC for a MIMO setting was found to improve the performance of such backscatter system. Thus, the case when the RFID tag employs OSTBC, and the RFID reader simply employs the uniform query was investigated, and the general previously-published formulation for performance analysis, which is applicable to any sub-channels fading assumptions, was employed to study the SER performances for Hoyt sub-channels.

More specifically, a systematic analysis has been presented for Orthogonal STBCs in MIMO RFID channels under Hoyt fading. Based on this analysis, closed-form SER expressions were derived using the conditional MGF approach. In particular, using partial fraction expansion, exact and asymptotic forms of error rate expressions were obtained for two and four receiving antennas $(N = 2, 4)$.

The derived expressions cover some fading distribution models as special cases; in addition, they can be used for different modulation schemes including BPSK, BFSK, ASK schemes. A very good agreement with previous studies was observed for the special case that the Hoyt fading covers. Additionally, from our analytical results several interesting properties of the channel were observed. First, the diversity order is solely determined by the number of tag antennas *L*. Second, the analytical results reveal that the SER of MIMO RF channel is much more sensitive to the channel condition of the forward links than that of the backscattering links.

The suitability of modeling a Hoyt-fading environment by a properly chosen Nakagami-m model, as far as the error performance of the OSTBC model under Hoyt fading is concerned, was also examined. The results have shown that the approximation of the Hoyt-fading environment with the equivalent Nakagami-m model always underestimates the performance of the Hoyt model.

6.2 Future Work

Currently, the SER performance is being analyzed for OSTBC in MIMO RFID channels undergoing Hoyt fading.

Eliminating our restricted Hoyt model assumptions (Reader receiving-antennas being equal 2 or 4) and extending the results to OSTBC under more general MIMO RFID fading channel such as $\alpha - \mu$ fading channel, are interesting future topics.

Acronyms and Abbreviations

AIDC: Automatic Identification and Data Capture

ASK: Amplitude-Shift Keying

BER   Bit Error Rate

BFSK: Binary Frequency Shift Keying

BPSK: Binary Phase Shift Keying

CW: Continuous Wave

EPC: Electronic Product Code

HF: High Frequency

LF: Low Frequency

LOS: Line-Of-Sight

MGF :   Moment-Generating Function

MIMO: Multiple-Input Multiple-Output

MRC :   Maximal Ratio Combining

NLOS: Non-Line-Of-Sight

OSTBC: Orthogonal Space-Time Block Code

PDF: Probability Density Function

RFID: Radio-Frequency Identification

SER: Symbol Error Rate

SNR: Signal-To-Noise Ratio

STBC: Space-Time Block Code

UHF: Ultra-High-Frequency

Notations

m:	Nakagami-m Distribution Severity Parameter
q:	Hoyt Distribution Severity Parameter
h:	Fading channel envelope
Ω:	Expectation of h^2, Variance
$f_h(h)$:	PDF of the fading channel envelope h
$I_0(.)$:	The zeroth-order modified Bessel function of the first kind
$\Delta(t)$:	The complex RF-tag antenna reflection coefficient.
M:	Reader-transmitting antennas
L:	Tag antennas
N:	Reader-receiving antennas
$\boldsymbol{r}(t)$:	The received signal from the $M \times L \times N$ dyadic channel
$\boldsymbol{x}(t)$:	The unmodulated signals transmitted from the reader
$\boldsymbol{n}(t)$:	The noises at the reader receivers
$\boldsymbol{H}^f$:	The channel matrix from the reader to the tag
$\boldsymbol{H}^b$:	The channel matrix from the tag to the reader
$\boldsymbol{S_I}(t)$:	The identical signaling (*backscattering*) matrix
$\boldsymbol{S_D}(t)$:	The diagonal signaling (*backscattering*) matrix
$\boldsymbol{S_F}(t)$:	The full signaling (*backscattering*) matrix
$\boldsymbol{H}$:	The channel matrix of the $N{\times}L$ channel
h_l^f:	The forward channels of the $N \times L$ channel, (l=1,…, L)
$h_{l,n}^b$:	The backscattering channels of the $N \times L$ channel, (l=1,…, L), (n=1,…,N)

$\boldsymbol{s}$:	The transmission symbols simultaneously transmitted from the tag antennas
$\mathcal{G}$:	The space-time encoding matrix
z_{ij}:	The modulated symbol to be transmitted in time slot i from antenna j.
c:	The code rate
$||.||_F$:	Frobenius norm of a matrix
E_b:	The average energy per bit
E_s:	The average energy per symbol
γ:	The instantaneous SNR per symbol
$\bar{\gamma}$:	The average SNR per symbol
R:	The symbol rate
g:	Modulation –dependent constant
$Q(.)$:	Gaussian Q function
$exp(.)$:	The exponential function
$\Gamma(.)$:	Gamma function
$\Gamma(.,.)$:	The incomplete Gamma function
$E_H(.)$:	The expectation over the density of H
π:	3.14159
$X|Y$:	The conditional random variable of X given Y
$G(\bar{\gamma})$:	The MGF of $||H||_F^2$
α_l:	The squared magnitude of the lth forward channel gain
$f_{\alpha_l}(\alpha_l)$:	PDF of α_l
$G_{h_{l,n}|\alpha_l}(\bar{\gamma})$:	The MGF of conditional distribution of $h_{l,n}$ on α_l
q_f:	The q factor of the forward channel
q_b:	The q factor of the backscattering channel

$\acute{r}$:   The received symbols that can be detected based on a simple maximum-likelihood method

$\acute{s}$:   The incoming symbols

w: The noises corresponding to the incoming symbols

d_a: The asymptotic diversity order

Bibliography

[1]   R. Want, "An introduction to RFID technology," *IEEE Pervasive Computing,* pp. 25-33, 2006.

[2]   F. Klaus, RFID Handbook :Fundamentals and Applications in Contantless Smart Cards and Identification, Wiley, 2003.

[3]   C. He and Z. Wang, "Unitary Query for the M x L x N MIMO Backscatter RFID Channel," *IEEE Transactions on Wireless Communications,* vol. 14, no. 5, May 2015.

[4]   C. He and Z. J. Wang, "Impact Of The Correlcation Between Forward And Backscatter Channels On RFID System Performance," in *IEEE International Conference on Acoustics ,Speech and Signal Processing*, 2011.

[5]   J. Mitsugi, "UHF band RFID Readability and Fading Measurements in Practical Propagation Environment," *Auto-ID Labs White Paper Series,* pp. 37-44, 2005.

[6]   J. Mitsugi and Y. Shibao, "Mutlipath Identification Using Steepest Gradient Method For Dynamic Inventory In UHF RFID," in *International Symposium on Applications and the Internet Workshops*, Hiroshima, Japan, 2007.

[7]   M. Polivka, M. Svanda and P. Hudec, "Analysis and Measurment of the RFID System Adapted For Identification of Moving Objects," in *36th European Microwave Conference*, 2006.

[8]   D. Kim, M. Ingram and W. Smith, "Measurments Of Small-scale Fading and Path Loss For Long Range RF Tags," *IEEE Trans. Antennas Propagation,* vol. 51, no. 8, pp. 1740-1749, 2003.

[9]   S. Benerjee, R. Jesme and R. Sainati, "Performance Analysis of Short Range UHF Propagation As Applicable To Passive RFID," in *IEEE International Conference on RFID*, Grapevine, TX, 2007.

[10]   S. Benerjee, R. Jesme and R. Sainati, "Investegation of Spatial and Frequency Diversity for Long Range UHF RFID," in *IEEE Antennas and Propagation Society International Symposium*, San Diego, CA, 2008.

[11]   J. Griffin and G. Durgin, "Gains for RF Tags Using Multiple Antennas," *IEEE Transactions on Antennas and Propagation ,* vol. 56, no. 2, pp. 563-570, 2008.

[12]   C. He and Z. Wang, "Closed-form BER Analysis Of Non-Coherent FSK in MISO Double Rayleigh Fading/RFID Channel," *IEEE Communications Letters ,* vol. 15, no. 8, pp. 848-850, 2011.

[13]   C. He, X. Chen, W. Su and Z. Wang, "On the Performce Of MIMO RFID Backscattering Channels," *EURASIP Journal on Wireless Communications and Networking,* vol. 11, pp. 1-27, 2012.

[14]   C. Boyer and S. Roy, "Space time Coding For Backscatter RFID," *IEEE Transactions on Wireless Communications ,* vol. 12, no. 5, pp. 2272-2280, 2013.

[15]   D. Kim, H. Jo, H. Yoon, C. Mun, B. Jang and J. Yook, "Reverse-link Interrogation Range Of A UHF MIMO-RFID System In Nakagami-m Fading Channels," *IEEE*

Transactions on Industrial Electronics, vol. 57, no. 4, pp. 1468-1477, 2010.

[16] C. He and Z. Wang, "SER of Orthogonal Space–Time Block Codes Over Rician and Nakagami- m RF Backscattering Channels," *IEEE Transactions on Vehicular Technology,* vol. 63, no. 2, pp. 654-663, 2014.

[17] M. Simon and M. Alouini, in *Digital Communication Over Fading Channels A Unified Approach to Performance Analysis*, Wiely -IEEE Press, 2004.

[18] D. Zogas, G. Karagiannidis and S. Kotsopoulos, "Equal Gain Combining Over Nakagami-m (Rice) and Nakagami-q (Hoyt) Generalized Fading Channels," *IEEE Transactions on Wireless Communications ,* vol. 4, no. 2, pp. 374-379, 2005.

[19] R. Radaydeh and M. Matalgah, "Non-Coherent Improved-Gain Diversity Reception Of Binary Orthogonal Signals In Nakagami-q (Hoyt) Mobile Channels," *IET Communications ,* vol. 2, no. 2, pp. 372-379, 2008.

[20] A. Jamoos and Y. Qabbani, "Performance Analysis of Orthogonal Space-time Block Codes Over Nakagami-q MIMO RFID Backscattering Channels," *Submitted to IET Communications ,* 2017.

[21] H. Stockman, "Communication by Means of Reflected Power," *Proceedings of the IRE , *vol. 36, no. 10, pp. 1196-1204, October 1948.

[22] R. Trujillo-Rasua, "Privacy in RFID and Mobile Objects," Tarragona, Spain, 2012.

[23] S. Roy and N. Karmakar, "Introduction to RFID Systems," in *Handbook of Smart Antennas for RFID Systems*, John Wiley & Sons, 2010, pp. 13-33.

[24] V. Girrulat, "Current state of the art benefits and challenges of RFID deployment in global supply chain," Dusseldorf, Germany, 2009.

[25] "EPC-RFID INFO - Item level Identification," Bar Code Graphics, 2017. [Online]. Available: http://www.epc-rfid.info/rfid_tags. [Accessed 20 March 2017].

[26] S.-S. Yeo and S. Kim, "Scalable and Flexible Privacy Protection Scheme for RFID Systems," in *Security and Privacy in Ad-hoc and Sensor Networks*, Visegrad, Hungary, 2005, p. 154.

[27] R. Trujillo-Rasua, "Privacy in RFID and Mobile Objects," Tarragona, Spain, 2012.

[28] P. Harliman, J. Lee, S. Kim and K. Jo, "Applying RFID Techniques for the Next-Generation Automotive Services," in *RFID Handbook. Applications, Technology, Security and Privacy*, United States of America, Taylor & Francis Group,, 2008, pp. 394-396.

[29] J. Griffin and G. Durgin, "Fading Statistics For Multi-antenna RF Tags," in *Handbook of Smart Antennas for RFID Systems*, John Wiley & Sons, Inc., 2010, pp. 469-470.

[30] J. Griffin and G. Durgin, "Link Budgets for Backscatter Radio Systems," in *Handbook of Smart Antennas for RFID Systems*, John Wiley & Sons, Inc., 2010, p. 451.

[31] D. Cassiloi, M. Win and A. Molisch, "The Ultra-Wide Bandwidth Indoor Channel :From Statistical Model To Simulations," *IEEE Sel. Areas Commun,* vol. 20, no. 6, pp.

1247-1257, 2002.

[32] D. Dardari, R. D`Errico, C. Roblin, A. Sibille and M. Z. Win, "Ultrawide Bandwidth RFID : The Next Generation," *Proc. IEEE,* vol. 98, pp. 1570-1582, 2010.

[33] M. Nakagami, "The m- distribution - A General Formula Of Intensity Distribution Of Rapid Fading," in *Statistical Methods In Radio Wave Propagation* , Oxford , UK, W.G.Hoffman Ed., 1960.

[34] N. Youssef and C. Wang, "A Study on the Second Order Statistics of Nakagami-Hoyt Mobile Fading Channels," *IEEE Transactions on Vehicular Techology,* vol. 54, no. 4, 2005.

[35] H. Shah, Performance Analysis of Space-Time Codes, Dallas, 2003.

[36] P. Sotica and E. Larsson, Space-Time Block Coding for Wireless Communications, Cambridge: Cambridge University Press, 2003.

[37] M. Ingram, M. Demirkol and D. Kim, "Transmit Diversity and Spatial Multiplexing for RF Links Using Modulated Backscatter," in *The International Symosium Signals , Systems , and Electronics*, Tokyo, Japan, 2001.

[38] H. Abderrazak, B. Slaheddine and B. Ridha, "A Transponder Anti-Collision Algorithm," in *Information and Communication Technologies Conference*, Damascus, Syria, 2006.

[39] D. Hanel, W. Burgard, D. Fox, K. Fishkin and M. Philipose, "Mapping and Localization with RFID Technology," in *IEEE International Conference on Robotics and Automation*, New Orleans, LA, USA, 2004.

[40] J. Wang, M. Amin and Y. Zhang, "Signal and Array Processing Technique for RFID readers," in *SPIE, Wireless Sensing and Processing*, 2006.

[41] M. Mi, M. Mickle, C. Capelli and H. Swift, "RF Energy Harvesting with Multiple Antennas in the Sampe Space," *IEEE Antennas and Propogation Magazine,* vol. 47, no. 5, pp. 100-106, 2005.

[42] L. Chiu, T. Yum, W. Chang, Q. Xue and C. Chan, "Retrodirective Array for RFID and Micowave Trcking Beacon Applications," *Micowave and Optical Technology Letters,* vol. 48, no. 2, pp. 409-411, 2006.

[43] H. Lehpamer, "Components of the RFID System," in *RFID Design Principles*, Artech House, 2012, p. 132.

[44] B. Shao, "Fully Printed Chipless RFID Tags Towards Item-level Tracking Applications," Stockholm, Sweden, 2014.

[45] B. Jamali, "A Development Platform for SDR-Based RFID Reader," in *Handbook of Smart Antennas*, John Wiley & Sons,, 2010, pp. 130-131.

[46] F. Zheng and T. Kaiser, "A Space-time Coding Approach For RFID MIMO Systems," *EURASIP Jouranl on Embedded Systems,* no. 9, 2012.

[47] A. Rahim, N. Karmakar and K. Ahmed, "Blind Channel Estimation in MIMO for MC-CDMA," in *Handbook of Smart Antennas for RFID Systems*, John Wiley & Sons, Inc., 2010, p. 539.

[48] R. Prasad and F. Velez, "Wimax Networks : Techno-Economic Vision and Challenges," Springer Science & Business Media, 2010, pp. 429-431.

[49] J. Verlag, Complexity Aspects in Near Capacity MIMO Detection Decoding, 2007.

[50] C. Yuen, Y. Guan and T. Tjhung, Quasi-orthogonal Space-time Block Code, Imperial College Press, 2007.

[51] S. Alamouti, "A simple transmit diversity technique for wireless communications," *IEEE Journal on Selected Areas in Communications,* vol. 16, no. 8, pp. 1451-1458, 1998.

[52] V. Tarokh, H. Jafarkhani and A. Calderbank, "Space-time block coding for wireless communications: performance results," *IEEE Journal on Selected Areas in Communications,* vol. 17, no. 3, pp. 451-460, 1999.

[53] M. Simon and M. Alouini, "A Unified Approach To The Performance Analysis Of Digital Communicaton Over Generalized Fading Channels," *IEEE Proc,* vol. 86, no. 9, pp. 1860-1877, 1998.

[54] S. Sandhu and A. Paulraj, "Space-time Block Codes : A Capacity Perspective," *IEEE Commun. Lett.,* vol. 4, no. 12, pp. 384-386, 2000.

[55] Y. Gong and K. Letaief, "On The Error Probability Of Orthogonal Space-Time Block Codes Over Keyhole MIMO Channel," *IEEE Transactions on Wireless Communications ,* vol. 6, no. 9, pp. 3402-3409, 2007.

Appendix A

Evaluation of $P_{OSTBC}(\bar{\gamma})$

The PDF of the forward channel that follows the Nakagami-q distribution (normalized channel energy) is

$$f(\alpha_l) = \frac{1+q_f^2}{2q_f} e^{\frac{-\left(1+q_f^2\right)^2 \alpha_l}{4 q_f^2}} \sum_{m=0}^{\infty} \frac{1}{(m!)^2} \left(\frac{1-q_f^4}{8 q_f^2} \alpha_l\right)^{2m} \tag{A.1}$$

where the equality is given by the Taylor expansion of the modified Bessel function of the first kind (i.e., $I_0(\,.\,)$). the conditional MGF $G_l(\bar{\gamma}|\alpha_l)$ can be expanded as

$$G_l(\bar{\gamma}|\alpha_l) = \left(\left(1 + 2\,\alpha_l\,\bar{\bar{\gamma}} + \frac{q_b^2\,(2\,\alpha_l\,\bar{\bar{\gamma}})^2}{(1+q_b^2)^2}\right)^{\frac{-1}{2}}\right)^N \tag{A.2}$$

Therefore, averaging $G(\bar{\gamma}|\alpha_l)$ over the density of α_l gives:

$$G_l(\bar{\bar{\gamma}}) = \int_{\alpha_l=0}^{\infty} f(\alpha_l)\, G_l(\bar{\gamma}|\alpha_l)\, d\alpha_l$$

$$= \int_{\alpha_l=0}^{\infty} \frac{1+q_f^2}{2q_f} e^{\frac{-\left(1+q_f^2\right)^2 \alpha_l}{4 q_f^2}} \sum_{m=0}^{\infty} \frac{1}{(m!)^2} \left(\frac{1-q_f^4}{8 q_f^2} \alpha_l\right)^{2m} \left(1 + 2\,\alpha_l\,\bar{\bar{\gamma}} + \frac{q_b^2\,(2\,\alpha_l\,\bar{\bar{\gamma}})^2}{(1+q_b^2)^2}\right)^{\frac{-N}{2}} d\alpha_l$$

$$= \sum_{m=0}^{\infty} \frac{D_1 D_2^{2m}}{(m!)^2} \int_{\alpha_l=0}^{\infty} e^{-D_1^2 \alpha_l}\, \alpha_l^{2m}\, (1 + 2\,\alpha_l\,\bar{\bar{\gamma}} + D_3\,(\alpha_l\,\bar{\bar{\gamma}})^2)^{\frac{-N}{2}} d\alpha_l$$

$$\doteq \sum_{m=0}^{\infty} \frac{D_1 D_2^{2m}}{(m!)^2}\, F(\bar{\bar{\gamma}}) \tag{A.3}$$

where $k_f = q_f^2$, $k_b = q_b^2$, $k_1 = 1 + k_b$, $k_2 = 1 + k_f$, $D_1 = \frac{1+k_f}{2\sqrt{k_f}}$, $D_2 = \frac{1-k_f^2}{8 k_f}$ and $D_3 = \frac{4 k_b}{(1+k_b)^2}$.

Case 1: = 2 :

$$F(\bar{\bar{\gamma}}) = \int_{\alpha_l=0}^{\infty} e^{-D_1^2 \alpha_l}\, \alpha_l^{2m}\, (1 + 2\,\alpha_l\,\bar{\bar{\gamma}} + D_3\,(\alpha_l\,\bar{\bar{\gamma}})^2)^{-1} d\alpha_l$$

$$= \int_{\alpha_l=0}^{\infty} e^{-D_1^2 \alpha_l}\, \alpha_l^{2m}\, \frac{k_1}{(k_b-1)} \left(\frac{k_b}{(k_1+2 k_b\,\bar{\bar{\gamma}}\,\alpha_l)} - \frac{1}{(k_1+2\,\bar{\bar{\gamma}}\,\alpha_l)}\right) d\alpha_l$$

$$= \int_{\alpha_l=0}^{\infty} e^{-D_1^2 \alpha_l} \alpha_l^{2m} \frac{k_1}{(k_b-1)} \left(\frac{k_b}{(k_1+2 k_b \bar{\bar{\gamma}} \alpha_l)} \right) d\alpha_l \; - \; \int_{\alpha_l=0}^{\infty} e^{-D_1^2 \alpha_l} \alpha_l^{2m} \frac{k_1}{(k_b-1)} \left(\frac{1}{(k_1+2 \bar{\bar{\gamma}} \alpha_l)} \right) d\alpha_l$$

$$=$$

$$\left(\frac{k_b}{(k_b-1)} (D_1^2)^{-(2m+1)} \int_{y=0}^{\infty} \left(1 + \frac{2 k_b \bar{\bar{\gamma}}}{k_1 D_1^2} y \right)^{-1} e^{-y} y^{2m} dy \right) -$$

$$\left(\frac{1}{(k_b-1)} (D_1^2)^{-(2m+1)} \int_{y=0}^{\infty} \left(1 + \frac{2 \bar{\bar{\gamma}}}{k_1 D_1^2} y \right)^{-1} e^{-y} y^{2m} dy \right)$$

$$= \frac{(D_1^2)^{-(2m+1)}}{(k_b-1)} \left(k_b \int_{y=0}^{\infty} \left(1 + \frac{2 k_b \bar{\bar{\gamma}}}{k_1 D_1^2} y \right)^{-1} e^{-y} y^{2m} dy \right) - \left(\int_{y=0}^{\infty} \left(1 + \frac{2 \bar{\bar{\gamma}}}{k_1 D_1^2} y \right)^{-1} e^{-y} y^{2m} dy \right) \quad \text{(A.4)}$$

where partial fraction expansion is used to arrive to the second line , and change of variable to arrive to the forth line, $y = D_1^2 \alpha_l$. By letting $\dot{m} = 2m+1$ and $\dot{N} = 1$ the function $M(s, \dot{m}, \dot{N}) \doteq \int_{t=0}^{\infty} t^{\dot{m}-1} e^{-t} (1 + s t)^{-\dot{N}} dt$ can be used, that was well studied in [55] and has a closed form of

$$M(s, \dot{m}, \dot{N}) \doteq e^{\frac{1}{s}} s^{-\dot{N}} \sum_{k=0}^{\dot{m}-1} \binom{\dot{m}-1}{k} \left(-\frac{1}{s} \right)^{\dot{m}-k-1} \Gamma \left(k - \dot{N} + 1, \frac{1}{s} \right) \quad \text{(A.5)}$$

where $\Gamma(.,.)$ is the incomplete gamma function. Substitute (A.5) in (A.4) and (A.3) equation (4.13) is obtained for $N = 2$.

Proof of the asymptotic form: The asymptotic form can be obtained when only considering the terms associated with the lower terms of m in the exact form. This is because the lower order of the pdf of α_l determines the asymptotic performance when SNR is large. $M(s, \dot{m}, \dot{N})$ has an asymptotic form for large $\bar{\bar{\gamma}}$ [16]

$$M(s, \dot{m}, \dot{N}) \doteq \begin{cases} \frac{ln(s)}{s^{\dot{m}}} & \text{if } \dot{m} = \dot{N} \\ \frac{(\dot{m}-1)! \, (a-b-1)!}{(a-1)! \, s^b} & \text{if } \dot{m} \neq \dot{N} \end{cases} \quad \text{(A.6)}$$

where $a = \max(\dot{m}, \dot{N})$ and $b = \min(\dot{m}, \dot{N})$ .With $m = 0$, we have $\dot{m} = \dot{N} = 1$, and

$$F(\bar{\bar{\gamma}}) = \frac{(D_1{}^2)^{-(1)}}{(k_b-1)} \left(k_b\, M\left(\frac{2\,k_b\bar{\bar{\gamma}}}{k_1 D_1{}^2}, 1, 1 \right) - M\left(\frac{2\,\bar{\bar{\gamma}}}{k_1 D_1{}^2}, 1, 1 \right) \right)$$

$$\doteq \frac{(D_1{}^2)^{-1}}{(k_b-1)} \left(k_b\, \frac{ln\left(\frac{2\,k_b\,\bar{\bar{\gamma}}}{k_1 D_1{}^2} \right)}{\left(\frac{2\,k_b\,\bar{\bar{\gamma}}}{k_1 D_1{}^2} \right)} - \frac{ln\left(\frac{2\bar{\bar{\gamma}}}{k_1 D_1{}^2} \right)}{\left(\frac{2\bar{\bar{\gamma}}}{k_1 D_1{}^2} \right)} \right)$$

$$= \frac{k_1}{2\bar{\bar{\gamma}}(k_b-1)}\, ln(k_b) \tag{A.7}$$

Substitute the asymptotic form of $F(\bar{\bar{\gamma}})$ back to (A.3) we have the asymptotic form of $G_l(\bar{\bar{\gamma}})$ as

$$G_l(\bar{\bar{\gamma}}, m = 0) = \frac{D_1\,k_1\,ln(k_b)}{2(k_b-1)}\,\bar{\bar{\gamma}}^{-1} \tag{A.8}$$

For $m > 0$, we have $a = \max\left(\dot{m}, \dot{N} \right) = \dot{m}$, $b = \min\left(\dot{m}, \dot{N} \right) = \dot{N} = 1$ and

$$F(\bar{\bar{\gamma}}) = \frac{(D_1{}^2)^{-(2m+1)}}{(k_b-1)} \left(k_b\, M\left(\frac{2\,k_b\,\bar{\bar{\gamma}}}{k_1 D_1{}^2}, 2m+1, 1 \right) - M\left(\frac{2\,\bar{\bar{\gamma}}}{k_1 D_1{}^2}, 2m+1, 1 \right) \right)$$

$$= \frac{(D_1{}^2)^{-(2m+1)}}{(k_b-1)} \left(k_b\, \frac{(2m-1)!}{\left(\frac{2\,k_b\,\bar{\bar{\gamma}}}{k_1 D_1{}^2} \right)} - \frac{(2m-1)!}{\left(\frac{2\,\bar{\bar{\gamma}}}{k_1 D_1{}^2} \right)} \right) = 0$$

Therefore, we have $G_l(\bar{\bar{\gamma}}, m > 0) = 0$, and

$$G_l(\bar{\bar{\gamma}}) \doteq G_l(\bar{\bar{\gamma}}, m = 0) = \frac{D_1\,k_1\,ln(k_b)}{2(k_b-1)}\,\bar{\bar{\gamma}}^{-1} \tag{A.9}$$

Case 2: N = 4

$$F(\bar{\bar{\gamma}}) = \int_{\alpha_l=0}^{\infty} e^{-D_1{}^2\alpha_l}\, \alpha_l{}^{2m}\, \left(1 + 2\,\alpha_l\,\bar{\bar{\gamma}} + D_3\,(\alpha_l\,\bar{\bar{\gamma}})^2 \right)^{\frac{-4}{2}} d\alpha_l$$

$$= \frac{1}{(k_b-1)^3} \int_{\alpha_l=0}^{\infty} e^{-D_1{}^2\alpha_l}\, \alpha_l{}^{2m}\, \left(\frac{(k_b-1)k_1{}^2}{(k_1+2\bar{\bar{\gamma}}\,\alpha_l)^2} - \frac{k_b{}^2\,(1-k_b)k_1{}^2}{(k_1+2\,k_b\bar{\bar{\gamma}}\,\alpha_l)^2} + \frac{2k_b k_1}{(k_1+2\,\bar{\bar{\gamma}}\,\alpha_l)} - \frac{2k_b{}^2\,k_1}{(k_1+2\,k_b\,\bar{\bar{\gamma}}\,\alpha_l)} \right) d\alpha_l$$

$$= \frac{1}{(k_b-1)^3} \left(\begin{array}{l} \int_{\alpha_l=0}^{\infty} e^{-D_1{}^2\alpha_l}\, \alpha_l{}^{2m}\, \frac{(k_b-1)k_1{}^2}{(k_1+2\bar{\bar{\gamma}}\,\alpha_l)^2}\, d\alpha_l - \int_{\alpha_l=0}^{\infty} e^{-D_1{}^2\alpha_l}\, \alpha_l{}^{2m}\, \frac{k_b{}^2\,(1-k_b)k_1{}^2}{(k_1+2\,k_b\bar{\bar{\gamma}}\,\alpha_l)^2}\, d\alpha_l \\ + \int_{\alpha_l=0}^{\infty} e^{-D_1{}^2\alpha_l}\, \alpha_l{}^{2m}\, \frac{2k_b k_1}{(k_1+2\,\bar{\bar{\gamma}}\,\alpha_l)}\, d\alpha_l - \int_{\alpha_l=0}^{\infty} e^{-D_1{}^2\alpha_l}\, \alpha_l{}^{2m}\, \frac{2k_b{}^2\,k_1}{(k_1+2\,k_b\,\bar{\bar{\gamma}}\,\alpha_l)}\, d\alpha_l \end{array} \right)$$

$$= \frac{(D_1{}^2)^{-(2m+1)}}{(k_b-1)^3} \left(\begin{array}{l} (k_b-1)\int_{y=0}^{\infty}\left(1+\frac{2\,\overline{\overline{\gamma}}}{k_1 D_1{}^2}y\right)^{-2}e^{-y}\,y^{2m}\,dy - k_b{}^2(1-k_b)\int_{y=0}^{\infty}\left(1+\frac{2\,k_b\,\overline{\overline{\gamma}}}{k_1 D_1{}^2}\,y\right)^{-2}e^{-y}\,y^{2m}dy \\[4mm] + 2k_b\int_{y=0}^{\infty}\left(1+\frac{2\,\overline{\overline{\gamma}}}{k_1 D_1{}^2}y\right)^{-1}e^{-y}\,y^{2m}\,dy - 2k_b{}^2\int_{y=0}^{\infty}\left(1+\frac{2\,k_b\,\overline{\overline{\gamma}}}{k_1 D_1{}^2}y\right)^{-1}e^{-y}\,y^{2m}\,dy \end{array} \right)$$

$$(A.10)$$

where we use partial fraction expansion to arrive to the second line , and change of variable to arrive to

the forth line, $y = D_1{}^2 \alpha_l$. By letting $\dot{m} = 2m+1$ and $\dot{N} = 1$ or 2 depending on the power in each

term, we can again make use of the function $M(s, \dot{m}, \dot{N})$ in (A.5). Substitute (A.5) in (A.10) and (A.3)

we obtain (4.13) for $N = 4$.

Proof of the asymptotic form: For $m = 0$, we have $\dot{m} < \dot{N}$ for the first two terms of $F(\overline{\overline{\gamma}})$, and

$\dot{m} = \dot{N}$ for the rest .

$$F(\overline{\overline{\gamma}}) = \frac{(D_1{}^2)^{-(1)}}{(k_b-1)^3}\left(\begin{array}{l} (k_b-1)M\left(\frac{2\,\overline{\overline{\gamma}}}{k_1 D_1{}^2},1,2\right) - k_b{}^2(1-k_b)\,M\left(\frac{2\,k_b\,\overline{\overline{\gamma}}}{k_1 D_1{}^2},1,2\right) \\[3mm] +2k_b M\left(\frac{2\,\overline{\overline{\gamma}}}{k_1 D_1{}^2},1,1\right) - 2k_b{}^2 M\left(\frac{2k_b\,\overline{\overline{\gamma}}}{k_1 D_1{}^2},1,1\right) \end{array} \right)$$

$$= \frac{(D_1{}^2)^{-(1)}}{(k_b-1)^3}\left((k_b-1)\frac{1}{\left(\frac{2\,\overline{\overline{\gamma}}}{k_1 D_1{}^2}\right)} - k_b{}^2(1-k_b)\frac{1}{\left(\frac{2\,k_b\,\overline{\overline{\gamma}}}{k_1 D_1{}^2}\right)} + 2k_b\frac{\ln\left(\frac{2\overline{\overline{\gamma}}}{k_1 D_1{}^2}\right)}{\left(\frac{2\,\overline{\overline{\gamma}}}{k_1 D_1{}^2}\right)} - 2k_b{}^2\frac{\ln\left(\frac{2k_b\overline{\overline{\gamma}}}{k_1 D_1{}^2}\right)}{\left(\frac{2\,k_b\,\overline{\overline{\gamma}}}{k_1 D_1{}^2}\right)} \right)$$

$$= \frac{1}{(k_b-1)^3}\left(\frac{(k_b-1)\,k_1}{2\,\overline{\overline{\gamma}}} - \frac{k_b\,(1-k_b)k_1}{2\,\overline{\overline{\gamma}}} + \frac{k_b k_1}{\overline{\overline{\gamma}}}\ln\left(\frac{2\overline{\overline{\gamma}}}{k_1 D_1{}^2}\right) - \frac{k_b k_1}{\overline{\overline{\gamma}}}\ln\left(\frac{2\,k_b\overline{\overline{\gamma}}}{k_1 D_1{}^2}\right) \right)$$

$$= \frac{1}{(k_b-1)^3}\left(\frac{(k_b-1)\,k_1{}^2}{2\,\overline{\overline{\gamma}}} - \frac{k_b k_1 \ln(k_b)}{\overline{\overline{\gamma}}} \right)$$

$$= \left(\frac{k_1{}^2}{2\,(k_b-1)^2} - \frac{k_b k_1 \ln(k_b)}{(k_b-1)^3} \right)\overline{\overline{\gamma}}^{-1} \qquad (A.11)$$

Substitute the asymptotic form of $F(\overline{\overline{\gamma}})$ back to (A.3) we have the asymptotic form of $G_l(\overline{\overline{\gamma}})$ as

$$G_l(\overline{\overline{\gamma}}, m = 0) = D_1\left(\frac{k_1{}^2}{2\,(k_b-1)^2} - \frac{k_b k_1 \ln(k_b)}{(k_b-1)^3} \right)\overline{\overline{\gamma}}^{-1} \qquad (A.12)$$

For $m > 0$, we have $a = \max\,(\dot{m}, \dot{N}) = \dot{m}$, $b = \min\,(\dot{m}, \dot{N}) = \dot{N}$ and

$$F(\bar{\gamma}) = \frac{\left(D_1{}^2\right)^{-(2m+1)}}{(k_b-1)^3}\left(\begin{array}{c}(k_b-1)M\left(\dfrac{2\,\bar{\bar{\gamma}}}{k_1D_1{}^2},2m+1,2\right) - k_b{}^2(1-k_b)\,M\left(\dfrac{2\,k_b\,\bar{\bar{\gamma}}}{k_1D_1{}^2},2m+1,2\right)\\[2mm] + 2k_bM\left(\dfrac{2\,\bar{\bar{\gamma}}}{k_1D_1{}^2},2m+1,1\right) - 2k_b{}^2\,M\left(\dfrac{2k_b\,\bar{\bar{\gamma}}}{k_1D_1{}^2},2m+1,1\right)\end{array}\right)$$

$$= \frac{\left(D_1{}^2\right)^{-(2m+1)}}{(k_b-1)^3}\left((k_b-1)\frac{(2m-2)!}{\left(\frac{2\,\bar{\bar{\gamma}}}{k_1D_1{}^2}\right)^2} - k_b{}^2\,(1-k_b)\;\frac{(2m-2)!}{\left(\frac{2\,k_b\,\bar{\bar{\gamma}}}{k_1D_1{}^2}\right)^2} + 2k_b\frac{(2m-1)!}{\left(\frac{2\bar{\bar{\gamma}}}{k_1D_1{}^2}\right)} - 2k_b{}^2\,\frac{(2m-1)!}{\left(\frac{2k_b\bar{\bar{\gamma}}}{k_1D_1{}^2}\right)}\right)$$

$$= \frac{\left(D_1{}^2\right)^{-(2m+1)}}{(k_b-1)^3}\left(\begin{array}{c}(k_b-1)\left(D_1{}^2\right)^2\left(\frac{k_1}{2\bar{\bar{\gamma}}}\right)^2(2m-2)! - (1-k_b)\left(\frac{k_1}{2\,\bar{\bar{\gamma}}}\right)^2\left(D_1{}^2\right)^2(2m-2)!\\[2mm] + \frac{k_bk_1}{\bar{\bar{\gamma}}}D_1{}^2(2m-1)! - \frac{k_bk_1}{\bar{\bar{\gamma}}}D_1{}^2(2m-1)!\end{array}\right)$$

$$= \frac{D_1{}^{2-4m}}{(k_b-1)^2}\left(2\left(\frac{k_1}{2\bar{\bar{\gamma}}}\right)^2(2m-2)!\right)$$

$$= \frac{D_1{}^{2-4m}}{2(k_b-1)^2}\left(k_1{}^2(2m-2)!\right)\bar{\bar{\gamma}}^{-2} \tag{A.13}$$

Therefore, we have

$$G_l(\bar{\bar{\gamma}},m>0) = \sum_{m=1}^{\infty}\frac{D_1D_2{}^{2m}}{(m!)^2}\left(\frac{D_1{}^{2-4m}}{2(k_b-1)^2}\left(k_1{}^2(2m-2)!\right)\bar{\bar{\gamma}}^{-2}\right)$$

$$= \bar{\bar{\gamma}}^{-2}\sum_{m=1}^{\infty}\frac{D_1{}^{3-4m}D_2{}^{2m}}{2(m!)^2}\left(\frac{k_1}{k_b-1}\right)^2(2m-2)!$$

The terms for m > 0 can be ignored since $G_l(\bar{\bar{\gamma}},m=0) = o(\bar{\bar{\gamma}}^{-1}) \gg o(\bar{\bar{\gamma}}^{-2})$ for large SNR.

$$G_l(\bar{\bar{\gamma}}) \doteq G_l(\bar{\bar{\gamma}},m=0) = D_1\left(\frac{k_1{}^2}{2\,(k_b-1)^2} - \frac{k_bk_1\ln(k_b)}{(\,k_b-1)^3}\right)\bar{\bar{\gamma}}^{-1} \tag{A.14}$$

تحليل أداء نظام الترميز في الفراغ والزمن لقنوات اضمحلال من نوع ناكاجامي-كيو في نظام متعدد المدخلات والمخرجات لتحديد الهوية باستخدام موجات الراديو.

إعداد: ياسمين هشام توفيق قباني

إشراف: د. علي جاموس

الملخص

تحديد الهويّة باستخدام موجات الراديو (RFID) هي تقنيّة أوتوماتيكيّة لتحديد الهوية تستخدم المجالات المغناطيسية للموجات الراديويّة في تحديد هويّة كائنات تحمل رقاقات تعريف موجودة داخل نطاق القراءة لجهاز القراءة والإرسال الخاصّ. تحديد الهوية هكذا عبر قناة لاسلكيّة لا يتطلّب بالضرورة كون البطاقة والقارئ في اتصال مباشر أو مصطفة بخط مستقيم .

هذه الخاصية المميّزة في نقل معلومات تحديد الهويّة لاسلكيًّا قد تؤثر سلباً على أداء هذا النظام، لأنّه وحتّى في حال وجود مسار اتصال مباشر، يبقى الاضمحلال موجوداً كون عمليّة التحديد تكون بمنطقة داخليّة وليست بالفراغ وبسبب بيئة القارئ المشوّشة، والطبيعة غير المتجانسة للكائنات المطلوب تحديد هويّتها. للتخفيف من مشكلة الاضمحلال هذه ولزيادة موثوقية القراءة ، تم اقتراح وتوظيف الترميز الكتلي في الفراغ والزمن لأنظمة تحديد الهويّة متعددة المدخلات و المخرجات.

في هذه الأطروحة، تمّ عمل دراسة تحليليّة لأداء نظام الترميز الكتلي في الفراغ والزمن في نظام متعدّد المدخلات والمخرجات يعتمد على رقاقات سلبيّة خاملة في تحديد الهوية باستخدام موجات الراديو. بصورة أكثر تخصيصاً، قمنا بتوظيف نهج الدالة المولّدة للعزوم في تحليل أداء نظام الترميز الكتلي المتعامد في الفراغ لنظام تحديد هويّة متعدد المدخلات والمخرجات لقنوات تشتّت يعتمد فيها الخبو على نظام (Nakagami-q). تم اشتقاق معادلات دقيقة وأخرى تقريبيّة لمعدل خطأ الرمز في حال استخدام هوائيين اثنين أو أربعة هوائيات للاستقبال عند القارئ .

تم مناقشة عدد من الخصائص المميزة لقناة الاضمحلال في هذا النظام، أهمّها: معدل التنوّع المحقّق، وتأثير كل من الوصلات أو القنوات الأماميّة و الخلفيّة على معدل الخطأ . وتم ملاحظة توافق مع النتائج المنشورة سابقاً في بعض الحالات الخاصّة للاضمحلال التي يشملها نظام (Nakagami-q) ضمنه.